https://doi.org/10.1016/j.ress.2023.109889

LINK CRITICALITY INDEX: REFINEMENT, FRAMEWORK EXTENSION, AND A CASE STUDY

Daniyar Kurmankhojayev [a], Guoyuan Li [a], Anthony Chen [a *]

[a] Department of Civil and Environmental Engineering

The Hong Kong Polytechnic University, Hung Hom, Hong Kong

*Corresponding author: anthony.chen@polyu.edu.hk

Abstract

The link criticality index (LCI) is a network performance-based measure that assesses criticality of network links based on flow fluctuations during traffic assignment. Unlike other network performance-based methods, LCI does not require link removal or multiple traffic assignments, and can account for topology, redundancy, congestion, and traveler behavior. However, the original LCI is based on a deterministic user equilibrium (UE) framework, which may lead to two issues: (i) a link's criticality index can be affected by origin-destination (O-D) pairs even if their demand is routed away from the link and (ii) identical links can be ranked unequally. In this paper, we suggest a refinement to the functional form of LCI to cater to analysts who prefer to work within the UE framework; and we extend the LCI measure to stochastic user equilibrium (SUE) and SUE with elastic demand (ED). These extensions resolve the issues related to UE-based LCI and add to the behavioral realism of the network model. To demonstrate validity of concept, the resulting LCI measure is applied to assess the criticality of bridges in Winnipeg, Canada. The obtained results are reasonable and consistent with the previous methods based on the full-network scan approach.

Keywords: Vulnerability analysis; Link criticality index; Stochastic user equilibrium; Demand elasticity.

1. INTRODUCTION

1.1. Background and motivation

Road transport networks play a vital role in the daily lives of people living in cities around the world, providing access to essential services, promoting environmental sustainability, fostering social connections, and supporting economic growth *[1, 2]*. A transport network, however, can be vulnerable to various natural and/or man-made disasters, which may result in failure or decrease of service level of transport network assets *[3, 4, 5]*. Failure or decrease of service level of a transport network asset may disrupt or degrade a transport system's functionality causing large economical and societal losses *[6, 7, 8]*. Moreover, some network assets may be more important than others. The more critical the asset, the more severe the negative impact on the system may be when that asset is disrupted. By identifying the critical infrastructure elements and developing contingency policies and/or emergency plans, the consequences of network disruptions can be substantially reduced *[9, 10, 11]*. Criticality rankings can help policy makers to allocate resources and devise recovery plans before and after disruptions, respectively, to enhance network resilience. This makes the critical link identification problem of road transport networks an area of interest to transport authorities and researchers.

Road transport networks can accommodate different travel modes, such as private vehicles *[12]*, transit *[13]*, bicycles *[14]*, and pedestrians *[15]*, each with its own behavioral features that affect how it uses the network. We limit our scope to the private vehicle mode, which is the most common and dominant travel mode in most cities *[16]*. One of the key aspects of analyzing private vehicle networks is traffic assignment (TA), which is the process of allocating the travel demand to the network links based on the travel costs and preferences of the travelers. TA determines the flow and travel time patterns of the network, which can be used to calculate various network performance measures (e.g., congestion level as an efficiency indicator) *[17]*. TA is also crucial for analyzing the criticality of the network links *[18]*, which is the main objective of this paper. If the criticality of a link is based on TA, it may objectively reflect how much the network performance would degrade if links were removed or disrupted.

To identify critical links in transport networks, a common method is to use a full network scan method based on the TA analysis *[9, 12, 19]*. This method measures the network-wide impact of each link by iteratively removing (or degrading capacity of) the link and solving the TA problem. The critical links are the ones that cause the most network performance drop when removed *[11]*. The full-scan method is consistent with the rationale of network users to minimize their travel costs and it is based on equilibrium flows, which considers the network's connectivity, travel demand, service level, and travelers' behavior *[12, 18, 19]*. However, this method is computationally costly, as it requires solving the TA problem for each link removal *[3, 18, 20]*. It makes the full-scan method impractical for real-world applications. Many *approximate methods (see [3], [21], [22])* have been proposed to address the computational burden associated with the full-scan method. Most of these methods try to "approximate" the full-scan method by obviating the scan for "unimportant" subsets of links *[21, 22]*, and some do it by reducing the impact area around degraded links while still scanning through all links *(see [3])*. Besides the approximate methods, there are also *heuristic methods*. These methods apply various heuristics to circumvent network scan by using the iterative information of the TA process to rank all network links *(see [18], [23])*. The LCI method in *Almotahari and Yazici [18]* is a distinct heuristic method that evaluates link criticality by their flow changes at each iteration of the TA process. This method considers topology and redundancy by

treating each link as part of composite structures such as O-D pairs and paths. It also accounts for congestion. LCI assigns higher criticality to a link that carries more flow despite increasing saturation, indicating that the link is more congested and more difficult to replace.

In this study, we refine, extend, and demonstrate validity of the improved LCI method. The original LCI *[18]* is based on a user equilibrium (UE) framework with fixed demand (FD). There are a few issues with this. First, UE assumes perfect perception of network travel times whereas the FD assumption may overlook the impact of other travel choices such as travel, destination, or mode choice on travel demand, resulting in travel costs that are unrealistically high *[24, 25, 26]*. Furthermore, the UE framework can yield zero-flow routes when used with a path-based solution algorithm, and zero-flow routes may lead to an overestimation of link criticality. Another drawback of the original UE-based LCI lies in the inconsistent ranking of identical links due to the all-or-nothing (AON) network loading procedure typical of the UE framework *[17]*. The AON procedure allocates O-D demand to the shortest path and disregards other identical routes. This issue may compromise the validity of the ranking. Motivated by the above challenges, this study aims to refine the functional form of the UE-based LCI to address the zero-flow problem, should an analyst opt to maintain the UE framework. Next, to eliminate the limitations of the UE framework with FD, we extend the analysis to stochastic user equilibrium (SUE) and SUE with elastic demand (ED). These relax the perfect perception of travel time assumption while naturally resolving all aforementioned issues and providing a more behaviorally realistic platform for assessing link criticality in a transportation network. Without the loss of generality, we adopt the SUE and SUE-ED formulations provided by *Fisk [27]* and *Yang and Bell [24]*, respectively. Both formulations use the multinomial logit (MNL) model, which is one of the simplest closed-form route choice models. To demonstrate validity of concept, we apply the enhanced LCI measure to several simplified toy networks and a real-size transportation network for assessing criticality of bridges in the city Winnipeg, Canada.

1.2. Literature review

Identification and ranking of critical transport network components serve as a typical first step in vulnerability, reliability, and resilience analyses in the context of road networks. Understanding the relation between these concepts may help to navigate in massive interdisciplinary literature published recently. *Liu and Song [1]* review the concept of resilience in the context of different critical infrastructure networks including transport networks. Reviews on vulnerability and resilience analysis of road transport networks are provided in *[28, 29, 30, 31]*. *Faturechi and Miller-Hooks [32]* and Gu et al. *[10]* discuss similarities and differences between these concepts. A comprehensive review of resilience concept in multi-modal transport network context is provided in *[33]*. Review of criticality analysis methods in road networks is provided in *[11]*.

Discrete choice and TA models are crucial for analyzing the criticality of the network links. Modeling route choice behavior entails various challenges, such as handling the large and diverse route choice set, accounting for route overlap, incorporating travel time uncertainty, and reflecting bounded rationality *[34]*, among others. Discrete choice theory is often used as the basis for route choice models. There is a considerable body of research on modeling physical path overlaps using discrete choice theory *[35, 36, 37]*. Numerous studies have investigated the challenges and opportunities of joint modeling choice set formation and route choice *(see [38])*. Travelers' bounded rationality has been the subject of

much research and debate in the context of route choice *(see [34, 39])*. A large and growing literature has tried to incorporate travelers' hierarchical perception of space into route choice modeling *(see [40, 41])*. Using route choice models as input, traffic assignment models could capture congestion effects on network performance under various scenarios, such as imperfect travel time perception *(see [12])*, demand elasticity *(see [26, 42])*, and emerging technologies *(see [43, 44])*. A more extensive discussion of the related work on route choice models and traffic assignment models can be found in *[34, 35]*.

Researchers have extensively studied the identification of critical links in transport networks. They have used pure topological metrics *[4, 45, 46]* and TA-based metrics *[9, 12, 19, 47]* to assess link criticalities. The former metrics did not account for demand and congestion effects on route choices, while the latter metrics did *[19]*. According to empirical studies, TA-based metrics are the most reliable metric for ranking link criticalities *(see [48])*. However, these metrics require the full network scan methodology based on TA, which is computationally intensive *[18]*. Many methods approximating the full-scan method have been proposed. These methods reduce the computational burden by scanning through a subset of links rather than a full link set *[21, 49, 50]*, limiting the impact area of a link failure while running a full network scan *[3]*, and scanning through equally sized link grids *[22, 51, 52]*. Although these approximate methods can substantially reduce the computational burden, they have their own limitations: (a) scanning through a subset of links may miss some critical links that are not in the subset, (b) limiting the impact area may ignore the global impact of link removal on other parts of the network, and (c) scanning through equally sized link grids may not capture the individual criticality of each link within the grid. In addition, these approximate methods require additional parameters, such as the size of the subset of links, the size of the impact area, or the size of the grid, respectively, to control computational time. Setting these parameters may be subjective and hence introduce some biases. Some methods eliminated network scan and ranked all links using just one TA with some heuristics. *Gauthier et al. [23]* measured link criticality with topological indices weighted by link travel time. This method ignored the impact of network degradation on link travel times. *Almotahari and Yazici [18]* proposed the LCI method to capture some of the behavioral phenomena that may occur due to link failures by using intermediate network flows to emulate the effect of network disruptions on link travel times. This method has several advantages over the approximate methods. First, LCI is robust to network size, as it does not need link removal or running multiple traffic assignments to rank all links in terms of criticality. Second, it does not need additional parameters. For these reasons, we see a potential in working with LCI for practical applications. The original LCI assumes a UE framework, enumerated path set, and used a path-based Frank-Wolfe (FW) algorithm to solve the traffic assignment problem. *Almotahari and Yazici [20]* improved the computational aspect of *[18]* by relaxing the assumption of an enumerated path set and using a more efficient path-based algorithm, but both studies *[18]* and *[20]* maintained the assumption of perfect perception of travel time and FD.

1.3. Objectives and contributions

In summary, the objectives and key contributions made in this paper are as follows:

1. **Refining the UE-based LCI**: The functional form of the UE-based LCI was enhanced to specifically tackle the challenge of zero-flow scenarios. This refinement was introduced to cater to analysts who prefer to work within the UE framework.

2. **Extension to SUE**: To overcome the limitations associated with the UE framework, the analysis was extended to SUE. This extension addressed issues like perfect perception of network travel time and naturally resolved zero-flow and inconsistent ranking of identical links problems.
3. **Extension to SUE with ED**: To better align the link criticality assessment platform with actual traveler behavior, real-world aspects such as demand elasticity were considered. The proposed modifications aimed to create a more accurate and behaviorally realistic framework for evaluating link criticality in transportation networks.
4. **Demonstrating validity of concept through an application**: To validate the efficacy of the enhanced approach, a practical demonstration was conducted. This involved applying the enhanced LCI to an actual transportation network in Winnipeg, Canada. The specific focus was on assessing the criticality of bridges within Winnipeg's road network.

The remainder of the paper is organized as follows. Section 2 introduces the methodology, including notation, traffic assignment model formulation, solution algorithm as well as original and refined LCI measures. Sections 3 and 4 present the numerical results and concluding remarks, respectively. Appendix A provides discussion on applicability of the ED extension in the context of link criticality assessment. Appendix B lists the criticality values and rankings for all bridges of the case study.

2. METHODOLOGY

In this section, we discuss the framework of LCI computation and introduce each component of the framework. Fig. 1 illustrates the overall methodology of computing LCI.

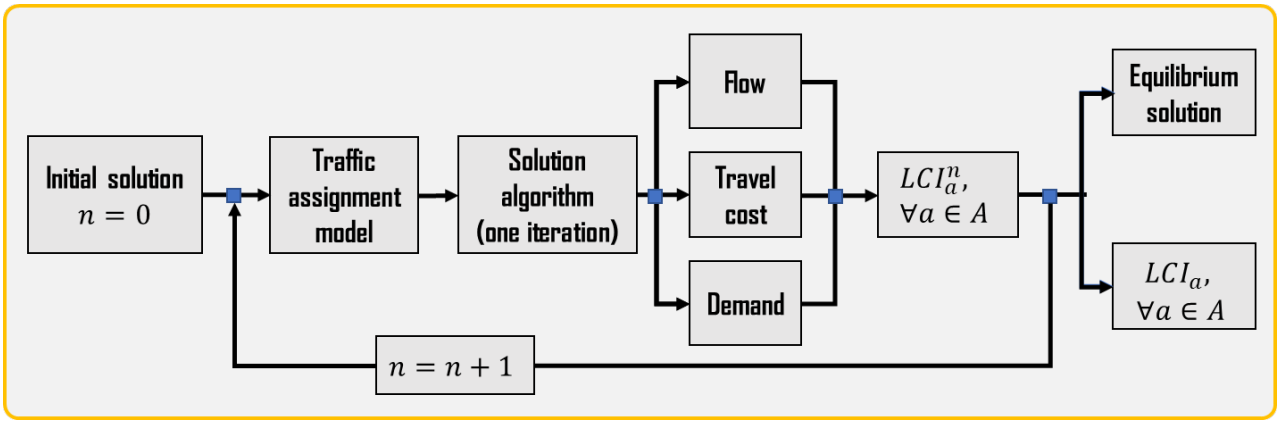

Figure 1. Methodology of link criticality index (LCI) computation.

As shown in Fig. 1, LCI ranks link criticality within a single traffic assignment without recalculating performance functions for each link removal. The idea behind LCI is to consider flow fluctuations of individual links during iterations of a solution algorithm. When a link is assigned more flow despite increasing saturation, the link is considered more critical for the network.

2.1. Notation

Table 1 provides a notation list.

Table 1. Notation.

Sets	
$\mathcal{N}$	*Set of nodes in the network*
$\mathcal{A}$	*Set of directed links*
$\mathcal{W}$	*Set of O–D pairs*
$\mathcal{R}^w$	*Set of routes connecting O–D pair w*
Parameters/inputs	
δ_{ar}^w	*Element of the path–link incidence matrix corresponding to an O–D pair w, path r, and link a*
θ	*Dispersion parameter of a route choice model*
ξ	*Demand function scaling parameter, which reflects the sensitivity of demand to travel cost*
$\overline{q}^w$	*Maximum (or potential) demand for O–D pair w*
Intermediate variables/functions	
$c_r^{w,n}$	*Deterministic travel time on path r of O–D pair w at iteration n*
$C_r^{w,n}$	*Perceived travel time on path r of O–D pair w at iteration n*
P_r^w	*Probability of choosing route r of O–D pair w*
x_a	*Flow on link a*
t_a	*Travel time on link a*
mc_a	*Marginal cost of traveling on link a*
D^w	*Demand function for O-D pair w*
Q	*Total network demand*
S_a^n	*Unweighted criticality score for link a at iteration n*
γ^w	*Demand-specific weight of O-D pairs w used in LCI*
$\mu_r^{w,n}$	*Path-specific weight for a path r of an O-D w at iteration n*
LCI_a	*Link criticality index for link a*
Decision variables	
f_r^w	*Flow on path r of O–D pair w*
q^w	*Demand of O–D pair w (for ED)*

2.2. Formulation

This section briefly introduces the multinomial logit (MNL) route choice model and the equivalent mathematical programming (MP) formulations.

2.2.1. Route choice models

The random utility model framework is a widely used and accepted framework for modeling route choice. It incorporates travelers' perception error in the random utility model, i.e.:

$$C_r^w = c_r^w + \varepsilon_r^w, \qquad \forall r \in \mathcal{R}^w, \forall w \in \mathcal{W} \tag{1}$$

where C_r^w is the perceived travel time on path r of O–D pair w, c_r^w is the deterministic travel time on path r of O–D pair w, and ε_r^w random error term.

It assumes that the perception error term, ε_r^w, is represented by the independently and identically distributed (IID) Gumbel random variable with the theoretical expectation $E[\varepsilon_r^w] = 0$ and

variance $Var[\varepsilon_r^w] = \frac{\pi^2\theta^2}{6}, \forall f \in \mathcal{R}^w$. The dispersion parameter θ measures the sensitivity of route choices with respect to travel cost *[17]*. The MNL model provides a closed-form probability expression, i.e.:

$$P_r^w = \frac{e^{-\theta c_r^w}}{\sum_{\forall l} e^{-\theta c_l^w}}, \quad \forall r \in \mathcal{R}^w, \forall w \in \mathcal{W} \tag{2}$$

Owing to the IID assumption, this model cannot consider (i) the similarity between travel alternatives and (ii) alternative-specific perception variances with respect to the heterogeneity of travel alternatives. However, it is sufficient for us to analyze the properties of LCI in the context of SUE. For more information on logit-based route choice models, interested readers may refer to *[35]*.

2.2.2. Equivalent mathematical programming formulations

In this study, we consider two formulations, namely MNL-SUE and MNL-SUE-ED. Both formulations satisfy the SUE conditions (3), and the MNL-SUE-ED formulation additionally satisfies the ED function (5).

$$f_r^w = P_r^w q^w, \qquad \forall r \in \mathcal{R}^w, \forall w \in \mathcal{W} \tag{3}$$

where f_r^w is flow on path r of O–D pair w, P_r^w is probability of choosing route r of O–D pair w, q^w is demand of O–D pair w.

The equivalent MNL-SUE and MNL-SUE-ED MP formulations are shown in Fig. 2.

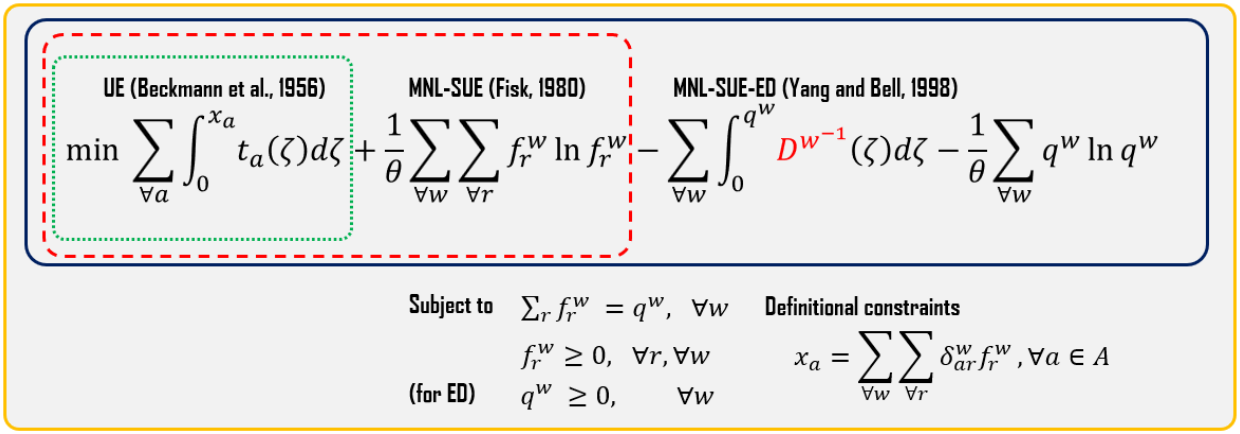

Figure 2. Equivalent mathematical programming (MP) formulation.

As shown in Fig. 2, the MP formulation for the MNL-SUE traffic assignment problem was developed by *Fisk [27]*, and it was extended by *Yang and Bell [24]* to MNL-SUE-ED. The objective function of the MNL-SUE-ED formulation has four terms. The first term is equivalent to the well-known Beckmann transformation objective function. The second term corresponds to the path-flow based entropy term. The third term is an inverse demand function term for the UE with ED problem. The fourth term represents the demand entropy term.

In the proceeding sections, we refer to MNL-SUE and MNL-SUE-ED as SUE and SUE-ED, respectively.

2.2.3. Demand function

Travel demand may be influenced by the level of service on the network. As congestion increases, travelers may decide to change their travel choices *[17]*. To address this phenomenon, travel demand between every O-D pair in the network can be assumed to be a function of level of service (LOS) in Eq. 4.

$$q^w = D^w(u^w), \qquad \forall w \in \mathcal{W} \tag{4}$$

where u^w is the expected perceived travel cost between O-D pair w. The demand function is monotonically decreasing in the O-D travel cost, bounded from above, and invertible. The inverse of the demand function is given in (5):

$$u^w = D^{w^{-1}}(q^w), \qquad \forall w \in \mathcal{W} \tag{5}$$

We can understand the reverse of the demand function as: the network user's travel benefits or the price they are ready to pay for their travel *[17]*.

2.3. Solution algorithm

This section presents the partial linearization method for solving the SUE and SUE-ED model. Fig. 3 provides a detailed procedure for implementing the partial linearization method to solve the SUE and SUE-ED problem.

The partial linearization method is a type of descent direction method used for continuous optimization problems *[53]*. It iteratively determines a search direction and step size until convergence is reached. To obtain the search direction, a partially linearized subproblem is solved using a first-order approximation of the first and third terms of the objective function (see Fig. 2). The algorithm for SUE and SUE-ED is similar, but for SUE-ED, the partial linearized subproblem needs to calculate travel demand based on the current route cost pattern to satisfy the elastic demand function as shown in Fig. 3.

The SUE-ED's objective function is quite complex (i.e., involving four summations: one over all links, one over all paths, and two over all O-D pairs) and hence computationally expensive to evaluate. To solve this, we use the self-regulated averaging (SRA) scheme proposed by *Liu et al. [54]* to determine an appropriate step size without the need to evaluate the objective function. SRA uses the residual error β and step size in the current iteration to determine the next step size and guarantees convergence with either $\lambda_1 > 1$ or $0 < \lambda_2 < 1$ controlling the decreasing speed. Refer to *[53]* for further information on the convergence properties of the partial linearization method.

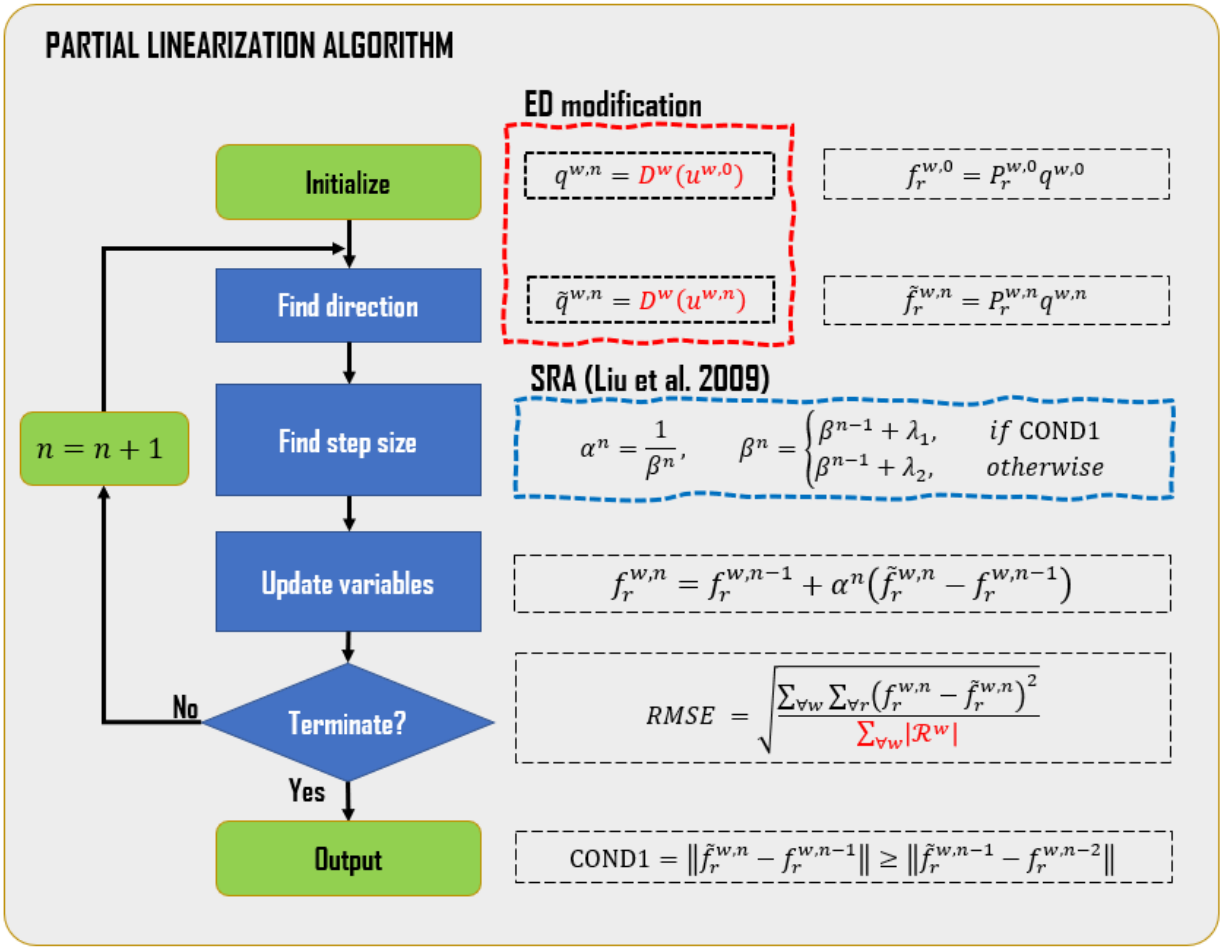

Figure 3. Partial linearization algorithm with self-regulated averaging (SRA) step size.

2.4. Link criticality index

In this section, we provide the original UE-based LCI *[18],* discuss its properties, elaborate on two deficiencies of the UE-based LCI, and propose three modifications that can help to overcome these deficiencies and make the LCI measure more realistic.

2.4.1. Original UE-based LCI

The LCI measure is presented in (6) – (10). It accounts for topology, redundancy, congestion, and travelers' behavior based on the UE framework. It uses link marginal cost (MC) to capture persistent flow assignment despite increasing congestion. If a saturated link is assigned additional flow between iterations n and $n + 1$, the travel time increase can be calculated as a product of link flow increment and MC in (7). MCs are normalized by link travel times for comparability. Two weighing coefficients account for links serving alternative paths (9) and multiple O-Ds (10).

$$LCI_a = \sum_{n=0}^{N-1} \sum_{\forall w} \sum_{\forall r} S_a^n \cdot \delta_{ra}^w \cdot \gamma^w \cdot \mu_r^{w,n}, \qquad \forall a \in A \tag{6}$$

where LCI_a is link criticality index for link a, S_a^n is unweighted criticality score for link a at iteration n, γ^w demand specific weight of O-D pairs w used in *LCI*, $\mu_r^{w,n}$ is path-specific weight for a path r of an O-D w at iteration n. The unweighted score and the weights can be computed as following:

$$S_a^n = \max([x_a^{n+1} - x_a^n], 1.0) \cdot \frac{mc_a(x_a^n)}{t_a(x_a^n)}, \qquad \forall a \in A, \forall n \in N \tag{7}$$

$$mc_a(x_a^n) = t_a(x_a^n) + x_a^n t_a'(x_a^n), \qquad \forall a \in A \tag{8}$$

$$\mu_r^{w,n} = \frac{1/c_r^{w,n}}{\sum_{\forall l} 1/c_l^{w,n}}, \qquad \forall r \in \mathcal{R}^w, \forall w \in \mathcal{W}, \forall n \in N \tag{9}$$

$$\gamma^w = \gamma^{w,n} = \frac{q^w}{Q}, \qquad \forall w \in \mathcal{W}, \forall n \in N \tag{10}$$

where $c_r^{w,n}$ is deterministic travel time on path r of O–D pair w at iteration n, x_a^n is flow on link a at iteration n, mc_a is marginal cost of traveling on link a, t_a is travel time on link a, *and* t_a' is the derivative of link travel time with respect to its flow.

Remark 1: The flow increments in each iteration are not based on behavioral phenomena, but on the purposes of the assignment methods. However, we would like to emphasize that this does not mean that the interim results are irrelevant or meaningless. On the contrary, interim results are arguably still consistent with the behavioral rationale of network users aiming to minimize their travel costs, which allows to assign higher criticality to a link that carries more flow despite increasing saturation, indicating that the link is more congested and more difficult to replace.

Remark 2: Different methods with different incremental properties might give different indices. However, this may not be a problem if the indices are consistent and comparable within each method. The purpose of the indices is to identify critical links and not to compare the methods directly.

Properties of components of LCI

Fig. 4 shows the properties of the O-D demand-based and path travel time-based weights of the LCI measure. As shown in Fig. 4 *(left)*, O-D pairs with higher travel demand have higher O-D weights than O-D pairs with lower travel demand. As shown in Fig. 4 *(right)*, the paths with longer travel times have lower weights than the paths with lower travel times.

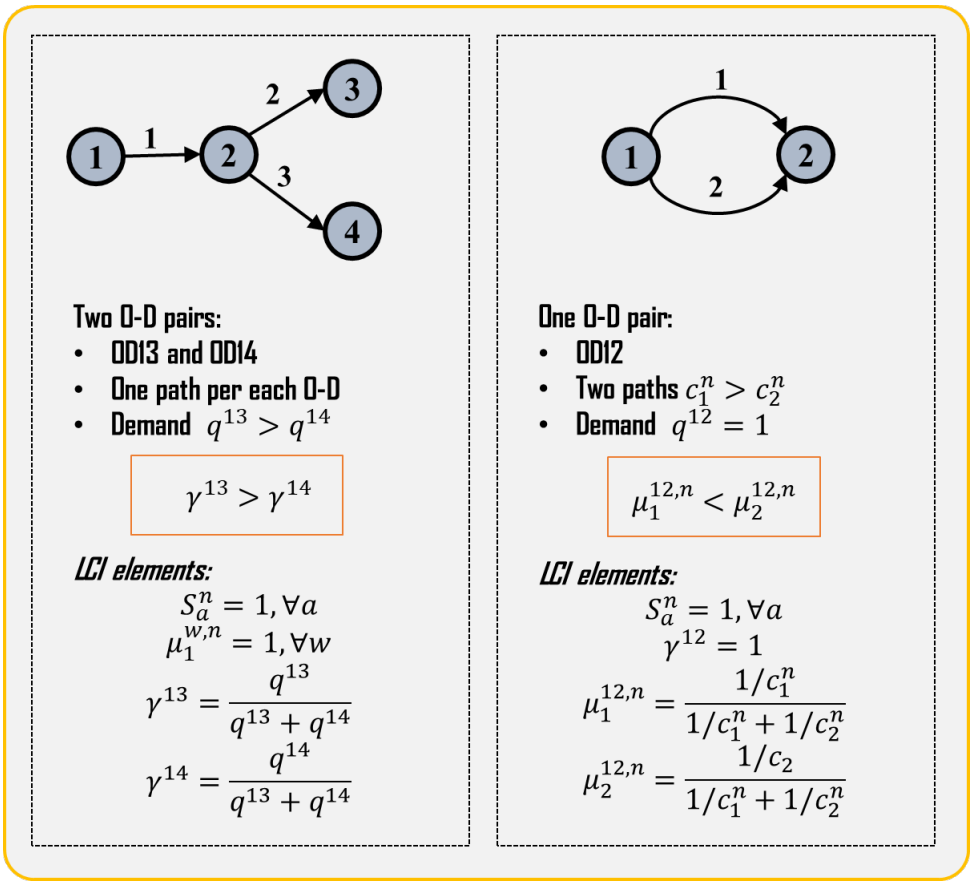

Figure 4. Properties of the O-D demand-based and path travel time-based weights of LCI.

Deficiencies of the original UE-based LCI

We observe two deficiencies of the original UE-based LCI, which may potentially make LCI biased: *(i) O-D's contribution to LCI when the link has no flow* and (ii) *identical links are ranked differently*. These issues are explained using the networks in Fig. 5 and Fig. 6, respectively.

O-D's contribution to LCI when the link has no flow[1]. The network in Fig. 5 has six links, two O-D pairs connected with two and three routes, respectively. The network is designed such that the demand of the first O-D (1,3) is served by Route 1 (i.e., Route 2 has zero flow), and the demand of the second O-D (1,4) is served by Route 4 and Route 5 (i.e., Route 3 has zero flow). The LCI value is computed for Link 1. At an iteration n, LCI_1^n is given as a sum of two terms, as shown in Fig. 5. Each term corresponds to a particular O-D pair. However, the second O-D pair should not contribute to LCI_1^n because Link 1 has no

[1] Arguably, this may be problematic if a path set, because of the limitations of path set generation algorithms, contains irrelevant (or unrealistic) alternatives, such as paths with long detours that may never be assigned any flow during the traffic assignment procedure. Being unrealistic, they are not expected to be in the path set so their O-D pairs should not contribute to the links' criticality. The original LCI cannot capture this nuance which may result in overestimation of link criticalities. On the other hand, any alternative path may also contribute to the redundancy of the network; hence, not including them may underestimate the criticality of a link rather than overestimate. Therefore, both views are legitimate depending on the purpose and network configurations, and it is up to the analysts to decide which view to consider based on the quality of their path sets.

flow from the second O-D pair. If we add the second term (Fig. 5), it artificially increases the criticality of the link, which may result in overestimation of its criticality. A formal solution to this example is provided in Section 3.1.

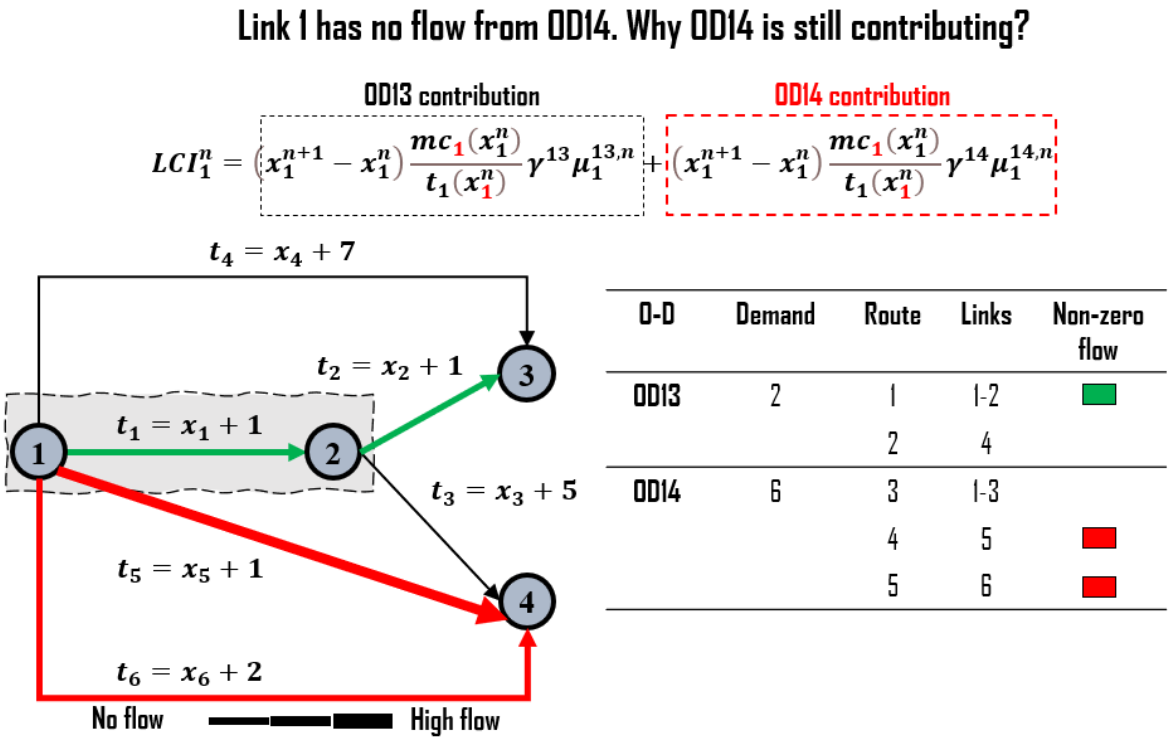

Figure 5. Two O-D pair network.

Identical links are ranked differently. The network in Fig. 6 has three links, a single O-D pair, and two routes. Link 1 and Link 2 are identical. Link 3 is shared by both routes. We mimic the solution process, compute LCI, and summarize the results in Table 2.

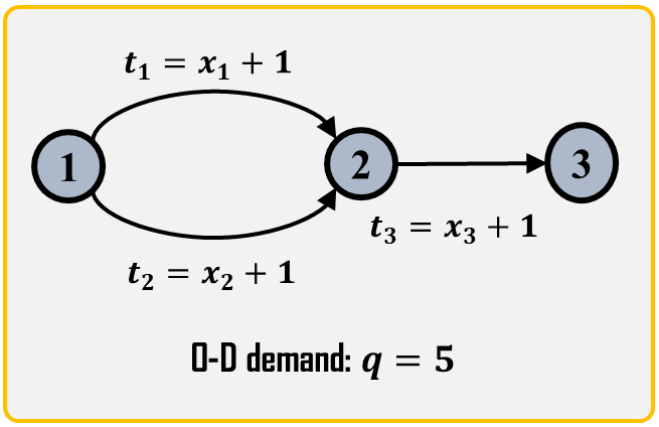

Figure 6. Three-link network (Link 1 and Link 2 are identical).

As shown in Table 2, Link 3 received the highest LCI. This was expected because Link 3 was included in both routes and was assigned flow equal to the full demand. If it were to be disrupted, then the O-D pair would be disconnected. Link 1 and Link 2 were expected to receive equal LCI values because they were identical, but they were assigned different values. Link 1 received a lower LCI value than Link 2.

Table 2. Process of equilibration and LCI computation.

Link	*1*				*2*				*3*			
	Iteration				*Iteration*				*Iteration*			
	1	*2*	*3*	*LCI*	*1*	*2*	*3*	*LCI*	*1*	*2*	*3*	*LCI*
Flow	*5*	*3*	*2.5*		*0*	*2*	*2.5*		*5*	*5*	*5*	
Time	*6*	*4*	*3.5*		*1*	*3*	*3.5*		*6*	*6*	*6*	
Marginal time	*1.83*	*1.75*	*1.71*		*1*	*5*	*6*		*1.83*	*1.83*	*1.83*	
γ	*1*	*1*	*1*		*1*	*1*	*1*		*1*	*1*	*1*	
μ	*0.37*	*0.47*	*0.5*		*0.63*	*0.53*	*0.5*		*1*	*1*	*1*	
Score	-	*1.83*	*1.75*		-	*2*	*1.66*		-	*1.83*	*1.83*	
LCI^n	-	*0.67*	*0.83*	***1.5***	-	*1.26*	*0.88*	***2.14***	-	*1.83*	*1.83*	***3.66***

This phenomenon occurred due to the initialization used in the UE framework. In UE, the initial solution and loading procedure is done using all-or-nothing (AON) assignment, which assigns the entire travel demand to the shortest path. Based on Table 2, since Link 1 is a part of the shortest path in the first iteration, it received high flow, while Link 2 received no flow. Consequent iterations equalized the flow but taking flow from Link 1 diminished its resulting LCI value and increased the LCI value of Link 2. Moreover, the score of LCI monotonically reduced with each iteration until equilibrium was reached. This suggests that initialization and the first few iterations play an important role in LCI calculation.

2.4.2. Refined LCI

This section outlines the refinements made to the original LCI to address the issues discussed in Section 2.4.1 and account for the framework extensions discussed in Section 2.2.

To address the first issue discussed in Section 2.4.1, we propose to split the score function (7) into two parts and substitute link flow increment by path flow increment, as shown in (11) – (12):

$$LCI_a = \sum_{n=0}^{N-1} \frac{mc_a(x_a^n)}{t_a(x_a^n)} \sum_{\forall w} \gamma^w \cdot z^{w,n} \sum_{\forall r} \mu_r^{w,n} \cdot \delta_{ar}^w, \qquad \forall a \in A \tag{11}$$

where the score function is split into two parts. The first part remains unchanged while the second part is substituted by a path flow increment $\left(f_k^{w,n+1} - f_k^{w,n}\right)$, i.e.:

$$z^{w,n} = \begin{cases} \sum_{\forall k} \left(f_k^{w,n+1} - f_k^{w,n}\right)\delta_{ak}^w, & if \sum_{\forall k} \left(f_k^{w,n+1} - f_k^{w,n}\right)\delta_{ak}^w > 0, \quad \forall w, \forall n \\ 1, & if \sum_{\forall k} \left(f_k^{w,n+1} - f_k^{w,n}\right)\delta_{ak}^w < 0, \quad \forall w, \forall n \\ 0, & if \nexists f_k^{w,n+1} \neq 0 \text{ and } \nexists f_k^{w,n} \neq 0, \quad \forall k, \forall w, \forall n \end{cases} \tag{12}$$

These changes can be interpreted as follows. The contribution of an O-D pair to the LCI is only considered if there is demand served from that pair. If all O-D pairs that a link serves have non-zero flow passing through that link, the refined LCI would be identical to the original LCI. This refinement of the functional form allows for a more precise consideration of O-D pairs in the LCI measure. It is worth noting that this modification may be unnecessary for LCI-SUE as the SUE framework assigns path flows based on positive probabilities and identical paths have equal probabilities. However, it can be particularly important in LCI-UE where zero-flow paths may exist.

The second issue discussed in Section 2.4.1 can be automatically alleviated by extending the traffic assignment problem to SUE. More importantly, another benefit of using the SUE framework is that it relaxes the assumption of perfect knowledge of travel time, and results in less bias solution. By extending the framework to SUE, we incorporate travelers' perception error into the model *[17]*, and load network according to a certain route choice model. Theoretically, all routes should have some non-zero flow. We substitute the actual path travel time by perceived path travel time in (9), i.e.:

$$\mu_r^{w,n} = \frac{1/C_r^{w,n}}{\sum_{\forall l} 1/C_l^{w,n}}, \qquad \forall r \in \mathcal{R}^w, \forall w \in \mathcal{W}, \forall n \in N \tag{13}$$

where $\mu_r^{w,n}$ is path-specific weight for a path r of an O-D w at iteration n and $C_r^{w,n}$ is the perceived travel time on path r of O-D w at iteration n.

Finally, the extension of the SUE framework to SUE-ED enables us to loosen the assumption of fixed demand and account for the potential influence of other travel choices that may affect travelers' behavior, resulting in a more realistic traffic assignment model. Demand elasticity results in variable O-D and total network demand. Consequently, the demand-based weight in (10) may vary from iteration to iteration.

In the following sections, we will use the abbreviations LCI-UE to refer to LCI based on UE, and LCI-SUE and LCI-SUE-ED to refer to LCI based on SUE and SUE-ED, respectively, for the sake of brevity.

3. NUMERICAL EXPERIMENTS

Three experiments were performed in this section. The first issue of the original LCI-UE (Section 2.4.1) was addressed by the refined LCI-UE in Experiment 1. LCI-UE and LCI-SUE were compared, and the second issue (Section 2.4.1) was resolved by LCI-SUE in Experiment 2. LCI-SUE-ED was also analyzed, and a sensitivity analysis of demand function parameters was conducted on the same network. Two real-size networks were used in Experiment 3 to compare the computation time of LCI for different traffic assignment models. Bridge criticality in the Winnipeg network, Canada, was also assessed and three LCI frameworks were compared with the index from *[12]*.

In all experiments except Experiment 1 (Section 3.1), the travel time of each link is assumed to follow the standard Bureau of Public Road (BPR):

$$t_a(x_a) = t_a^0 \left[1 + \alpha \left(\frac{x_a}{c_a}\right)^\beta\right], \qquad \forall a \in A \tag{14}$$

where t_a^0 is a free-flow travel time on link a; x_a is a flow on link a; c_a is the capacity of link a; α and β are exogenously defined parameters.

Without the loss of generality, in this study, the demand function is modeled using an exponential function of the expected perceived O–D travel cost (EPC), as follows:

$$D^w(u^w) = \overline{q}^w \cdot e^{-\xi u^w}, \qquad \forall w \in \mathcal{W} \tag{15}$$

where $\overline{q}^w$ is the maximum (or potential) demand for O–D pair $w \in \mathcal{W}$; ξ is the scaling parameter, which reflects sensitivity of demand to the travel cost.

To be able to compare the LCI values obtained based on different traffic assignment frameworks, we normalize the LCI values such that they lie in the range from 0 to 1, i.e.:

$$\widetilde{LCI}_a = \frac{LCI_a}{\sum_{\forall b} LCI_b}, \qquad \forall a \in A \tag{16}$$

and

$$\sum_{\forall a} \widetilde{LCI}_a = 1 \tag{17}$$

3.1. Experiment 1: Two O-D pair network

The purpose of this section is to compare the original LCI-UE with the refined LCI-UE, using the network illustrated in Fig. 5. To highlight the contrast between the original and refined LCI measures, we present the results only for a single arbitrary iteration n. The outcomes of this comparison are summarized in Table 3.

Table 3. An arbitrary iteration of the original LCI-UE and the refined LCI-UE.

	Components required for computation of LCI	*Original LCI*	*Refined LCI*
Target link	*Flow on Link 1 (n)*	*2*	
	Cost of Link 1 (n)	*3*	
	Marginal cost of Link 1 (n)	5	
	Flow on Link 1 (n+1)	*2*	
OD13	*Flow on Route 1 (n)*	*2*	
	Flow on Route 1 (n+1)	*2*	
	Flow on Route 2 (n)	*0*	
	Flow on Route 2 (n+1)	*0*	
	Cost of Route 1 (n)	*6*	
	Cost of Route 2 (n)	*7*	
OD14	*Flow on Route 3 (n)*	*0*	
	Flow on Route 4 (n)	*6*	
	Flow on Route 5 (n)	*0*	
	Cost of Route 3 (n)	*8*	
	Cost of Route 4 (n)	*7*	
	Cost of Route 5 (n)	*2*	
Weights	γ^{OD13} *(n)*	*0.25*	
	γ^{OD14} *(n)*	*0.75*	
	μ_1 *(n)*	*0.54*	
	μ_3 *(n)*	*0.21*	
	Score of Link 1 (n)	*1.67*	-
	LCI (n)	***0.49***	***0.23***

The results presented in Table 3 demonstrate that both the original LCI-UE and the refined LCI-UE require the same initial components for computation. However, the difference lies in the equation used to calculate the LCI value, where the original LCI-UE uses (6), i.e.:

$$LCI_1^n = \max([x_1^{n+1} - x_1^n], 1.0)\frac{mc_1(x_1^n)}{t_1(x_1^n)}\left[\gamma^{13}\mu_1^{13,n} + \gamma^{14}\mu_1^{14,n}\right]$$
$$= \max\big((2-2), 1.0\big) \cdot \frac{5}{3} \cdot [0.25 \cdot 0.54 + 0.75 \cdot 0.21] = 0.49$$

and the refined LCI-UE uses (11), i.e.:

$$LCI_1^n = \frac{mc_1(x_1^n)}{t_1(x_1^n)}\left[\gamma^{13}z^{13,n}\mu_1^{13,n} + \gamma^{14}z^{14,n}\mu_1^{14,n}\right] = \frac{5}{3}[0.25 \cdot 1 \cdot 0.54 + 0.75 \cdot 0 \cdot 0.21] = 0.23$$

The results show that the criticality value of the original UE-based LCI has more than twice higher value than the refined UE-based LCI.

It is important to note that this modification is relevant for UE-based LCI, where zero-flow paths may exist. However, for LCI-SUE or LCI-SUE-ED, this modification may not be necessary since the SUE framework assigns path flows based on probabilities, which theoretically should not result in zero-flow paths. Therefore, this modification is only needed for LCI-UE to ensure accurate assessment of link criticality.

3.2. Experiment 2: Loophole network

In this section, we use the loophole network to analyze LCI measures based on different traffic assignment frameworks. The loophole network is shown in Fig. 7.

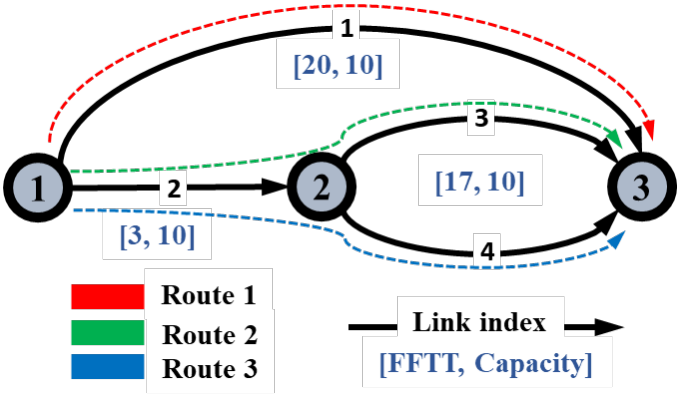

Figure 7. Loophole network.

The loophole network has four links and a single O-D pair connected by three paths with equal free-flow travel time. Routes 2 and 3 share Link 2. Moreover, they are identical. The parameters were set as follows: $\alpha = 0.15, \beta = 4$.

3.2.1. LCI-UE vs. LCI-SUE

In this section, we compare the original LCI-UE and LCI-SUE. The results are summarized in Table 4 and Fig. 8. As shown in Table 4, Link 2 was assigned the highest criticality value by both LCI-UE and LCI-SUE. It was followed by Link 1. Link 3 and 4 received the lowest values. This behavior was desired because Link 2 contributes more to route redundancy than any other link. It serves two routes, while the remaining links serve only one route each. If any of these links are disrupted, there will still be two routes available

to connect the given O-D pair. However, if Link 2 is disrupted, there will only be one alternative route available.

Table 4. Link criticality indices (LCI) and rankings for the loophole network ($q = 20, \theta = 0.5$).

Link	*LCI-UE*			*LCI-SUE*		
	LCI	*Normalized LCI*	*Rank*	*LCI*	*Normalized LCI*	*Rank*
1	*1608.95*	0.17	*2*	*3.15*	0.19	*2*
2	***5050.14***	***0.53***	***1***	***9.25***	***0.55***	***1***
3	*1403.61*	0.15	*3*	*2.19*	0.13	*3*
4	*1397.46*	0.15	*4*	*2.19*	0.13	*3*
Accuracy	*1e-5*			*1e-8*		
Iteration count	*3885*			*6*		

The reason why Link 2 was assigned a higher criticality value than Link 1 is that all components of the LCI for Link 2 (i.e., link flow, marginal-actual travel cost ratio, and path-based weights) were greater than the corresponding components for Link 1 (Fig. 8a - Fig. 8c), which resulted in higher criticality values at each iteration, as shown in (Fig. 8d).

From Table 2, it can also be noticed that the non-normalized values of LCI-UE and LCI-SUE differ in three orders of magnitude. It was because a non-normalized LCI depends on the number of iterations, and solving the UE problem required a substantially greater number of iterations than solving the SUE problem. For solving the UE and SUE problems, an SRA method and partial linearization method with the SRA step size were used, respectively. Due to the all-or-nothing network loading procedure, the SRA algorithm was much less efficient than the partial linearization algorithm, which uses a stochastic network loading procedure (3). Although the SRA algorithm may not be the most efficient algorithm for solving a UE problem, it is still sufficient for demonstrating the properties of LCI-UE

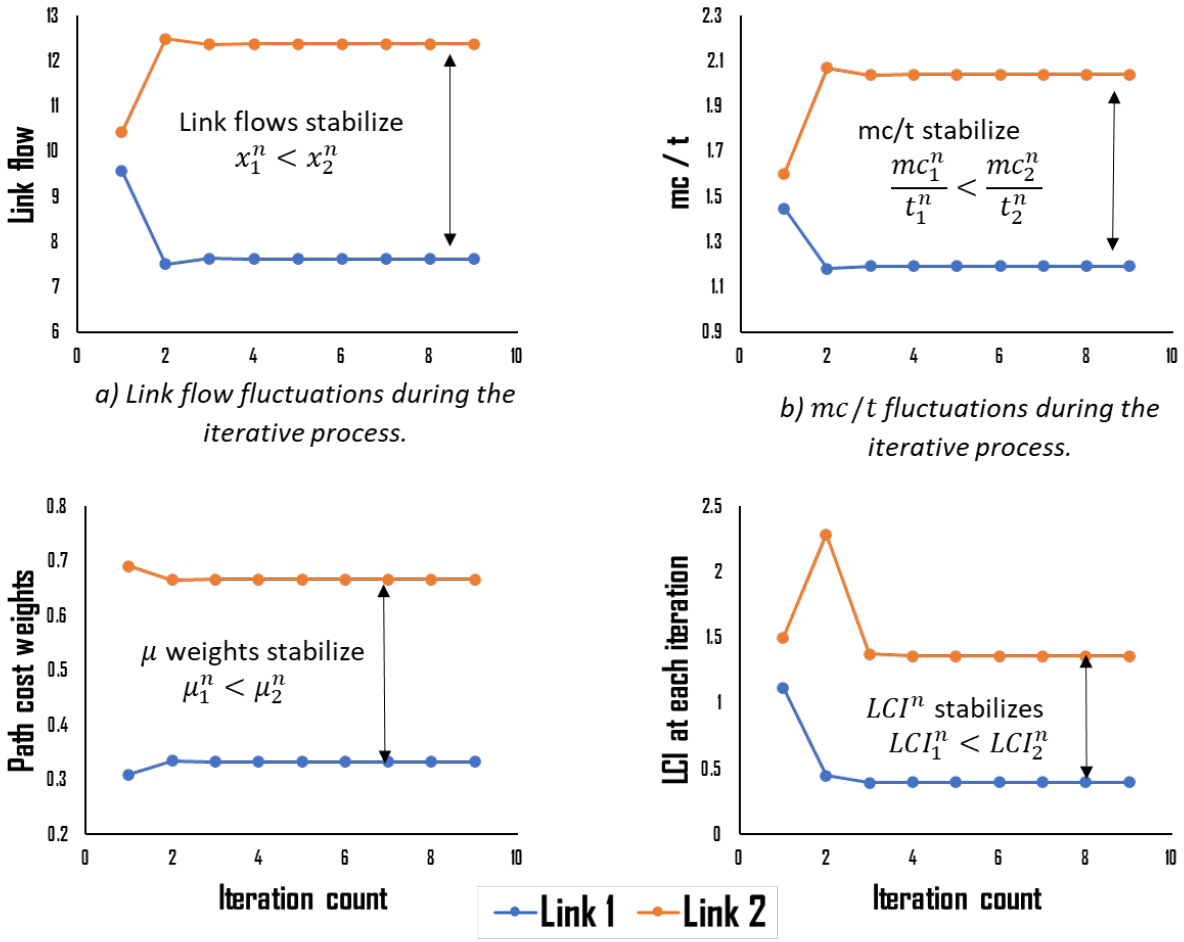

a) Link flow fluctuations during the iterative process.

b) mc / t fluctuations during the iterative process.

c) Fluctuations of path-based weights during the iterative process.

d) LCI at each iteration fluctuations during the iterative process.

Figure 8. Analysis of LCI-SUE fluctuations at each iteration. Link 2 obtains a higher LCI value than Link 1.

Sensitivity analysis

We conducted a sensitivity analysis with respect to travel demand and dispersion parameter. The results are summarized in Fig. 9 and Fig. 10, respectively. We analyzed the impact of demand level on criticality values of identical links by examining Link 3 and 4. These links were selected because we wanted to study the issue of initialization. Fig. 9a shows that at low demand values, identical links were assigned different LCI-UE values, but as demand increased, the differences in criticality values diminished. This can be attributed to three factors. Firstly, the first few iterations have the greatest impact, as demonstrated in Fig. 8. Secondly, the SRA algorithm requires fewer iterations to converge at lower demand levels than at higher demand levels. Finally, many iterations reduces the impact of the first few iterations because criticality values are summed up at each iteration. Fig. 9b demonstrates that LCI-SUE does not suffer from this issue, and identical links receive equal criticality values. This is because the stochastic network loading assigns non-zero flow to all alternatives in the path set, resulting in identical links receiving equal amounts

of flow (if not traversed by routes of other O-D pairs). An abrupt bend observed in Fig. 9b at demand level 20 potentially occurred due to reaching network capacity.

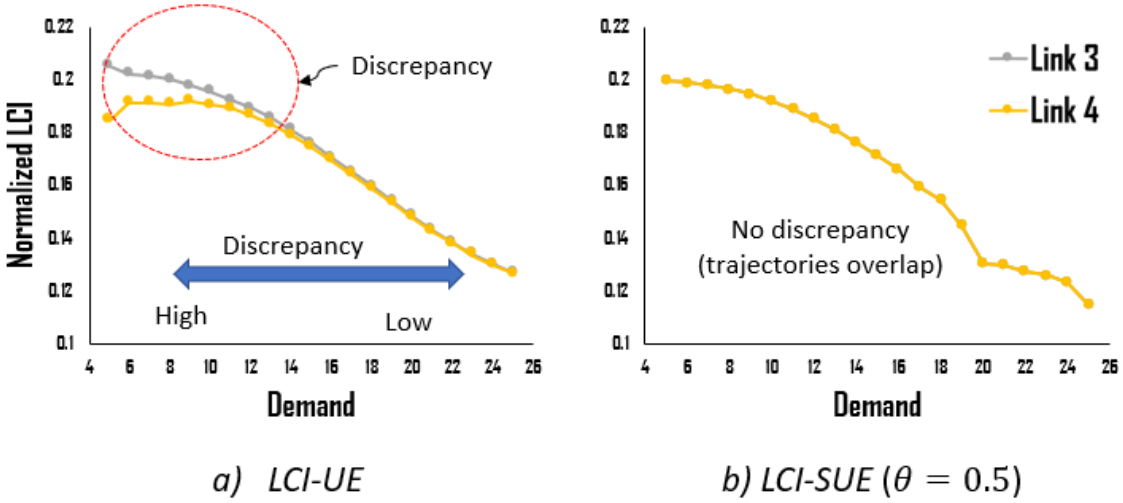

a) LCI-UE *b) LCI-SUE* ($\theta = 0.5$)

Figure 9. Discrepancy of LCI values of two identical links.

The impact of the dispersion parameter on LCI-SUE is analyzed. Results in Fig. 10 revealed that, at low dispersion parameter values, Links 1, 3, and 4 had similar LCI-SUE values. However, as the dispersion parameter value increased, Link 1 became consistently more critical than Link 3 and 4, indicating that it played a more important role in the network.

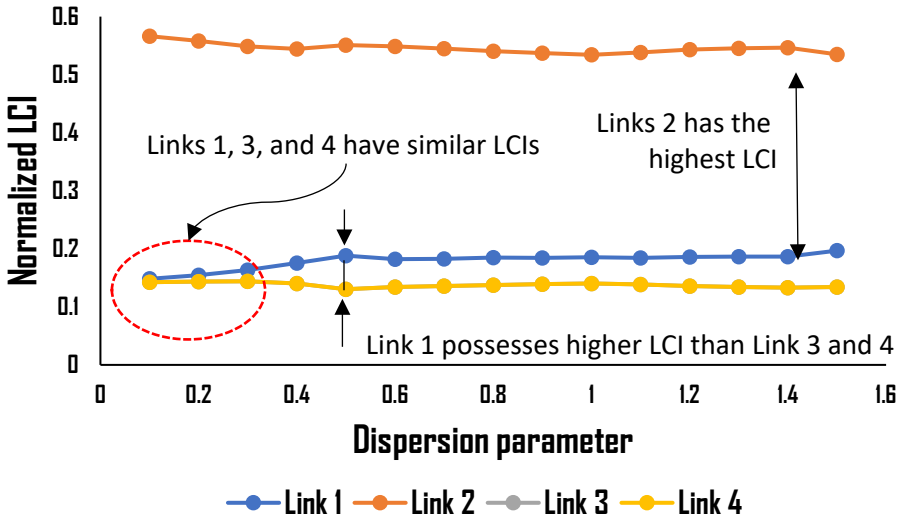

Figure 10. Impact of dispersion parameter on LCI-SUE ($q = 20$).

It is well known that when the dispersion parameter has low values, the model is less sensitive to travel time. As the dispersion parameter value increases, the equilibrium solution of a SUE problem becomes more and more sensitive to travel time, hence closer to the UE solution *[17]*. At certain iterations, Link 1's lower travel time allowed it to be assigned more flow, thereby increasing its importance over Links 3 and 4. Therefore, the model became sensitive enough to travel time changes, allowing it to differentiate the higher criticality of Link 1 compared to Links 3 and 4 as the dispersion parameter value increased over 0.4.

3.2.2. LCI-SUE vs. LCI-SUE-ED[2]

In this section, we compare LCI-SUE and LCI-SUE-ED. The results are summarized in Table 5 and Fig. 11 – Fig. 14. From Table 5, it is evident that the link rankings have remained unchanged. Link 2 has the highest rank, followed by Link 1, and then by Links 3 and 4 in that order. On the other hand, it should be noted that the LCI-SUE-ED value of Links 2 is slightly higher, while the LCI-SUE-ED values for Link 3 and 4 are slightly lower than their corresponding LCI-SUE values. Furthermore, the partial linearization algorithm converges in a relatively higher number of iterations in the case of LCI-SUE-ED than in the case of LCI-SUE.

Table 5. LCI-SUE and LCI-SUE-ED values for the loophole network ($q = 20, \theta = 0.5, \xi = 0.01, \bar{q} = 40$).

Link	*LCI-SUE*			*LCI-SUE-ED*		
	LCI	*Normalized LCI*	*Rank*	*LCI*	*Normalized LCI*	*Rank*
1	*3.15*	0.19	*2*	*68.81*	0.19	*2*
2	***9.25***	***0.55***	***1***	***217.97***	***0.59***	***1***
3	*2.19*	0.13	*3*	*41.54*	0.11	*3*
4	*2.19*	0.13	*3*	*41.54*	0.11	*3*
Accuracy	*1e-8*			*1e-8*		
Iteration count	*6*			*81*		

The reason why LCI-SUE-ED value of Link 2 was higher is related to the mechanism of changing demand. In SUE-ED, demand is a function of LOS. Specifically, when LOS is low, then the demand reduces, while when it is high, demand increases. From Fig. 11, we can see that the network demand fluctuated substantially during the first several iterations before it managed to stabilize.

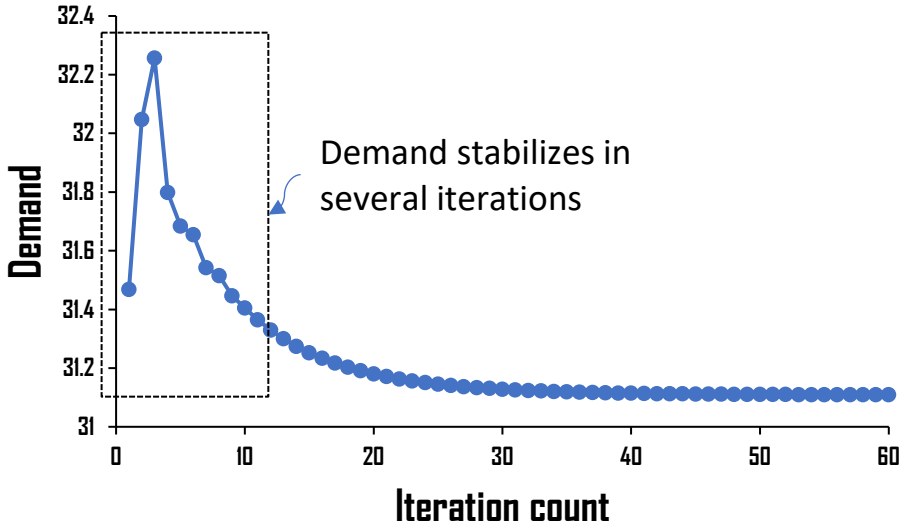

Figure 11. Demand changes during the iterative process.

[2] Readers can refer to Appendix A for a discussion on the feasibility of the ED extension for link criticality ranking.

From Fig. 12, we can see that this affected the flow on Link 2. It also fluctuated considerably during these iterations in the case of SUE-ED, especially during the first two iterations. In contrast, the flow on Link 2 remained relatively stable in the case of SUE, as shown in Fig. 12.

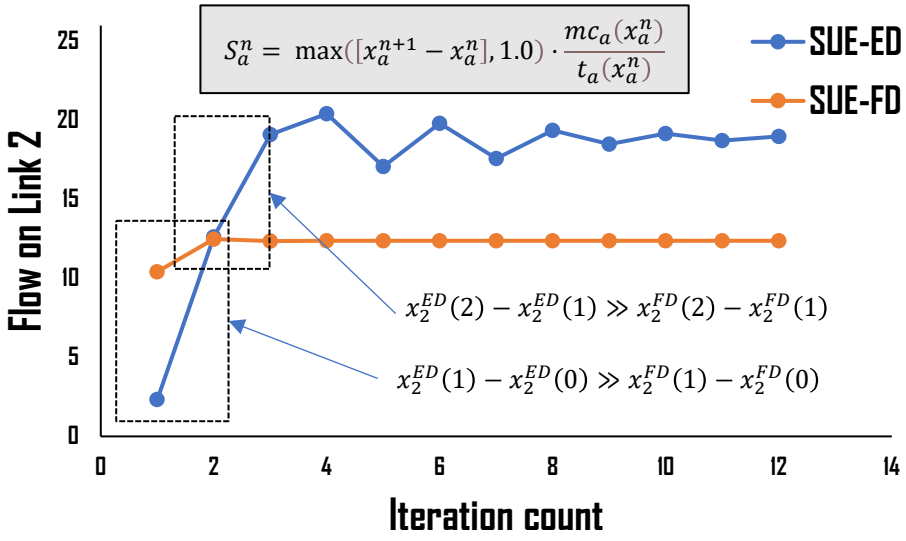

Figure 12. Flow fluctuations on Link 2 during the iterative process.

From Fig. 13, we can see why LCI-SUE-ED value of Link 1 did not grow. It happened because the flow on Link 1 was reducing the first few iterations, whereas the flow on Link 2 was increasing.

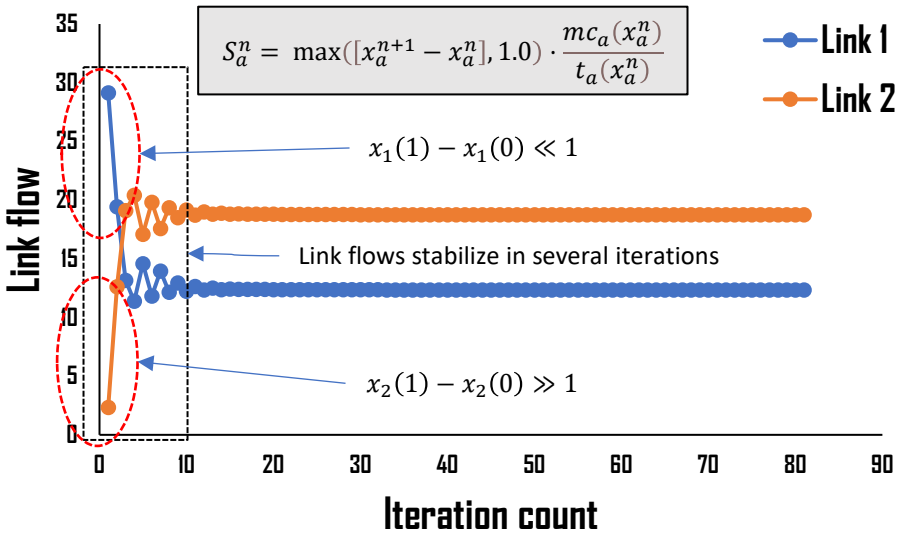

Figure 13. Link flow changes during the iterative process.

The reason why SUE-ED needed more iterations than SUE problem is that ED introduces additional non-linearity in the traffic assignment problem, making the problem more complex and challenging to solve. The iterative solution algorithms have to perform additional computations to accommodate this non-linearity, which may take more iterations to converge.

Sensitivity analysis

The demand function, which is represented by (15), has two parameters: the scaling parameter, ξ, and the maximum potential demand, $\bar{q}^w$. The sensitivity analysis for these two parameters is presented in Fig. 14a for the scaling parameter and Fig. 14b for the maximum potential demand. The results from Fig. 14 indicate that these parameters have a limited impact on the LCI-SUE-ED values.

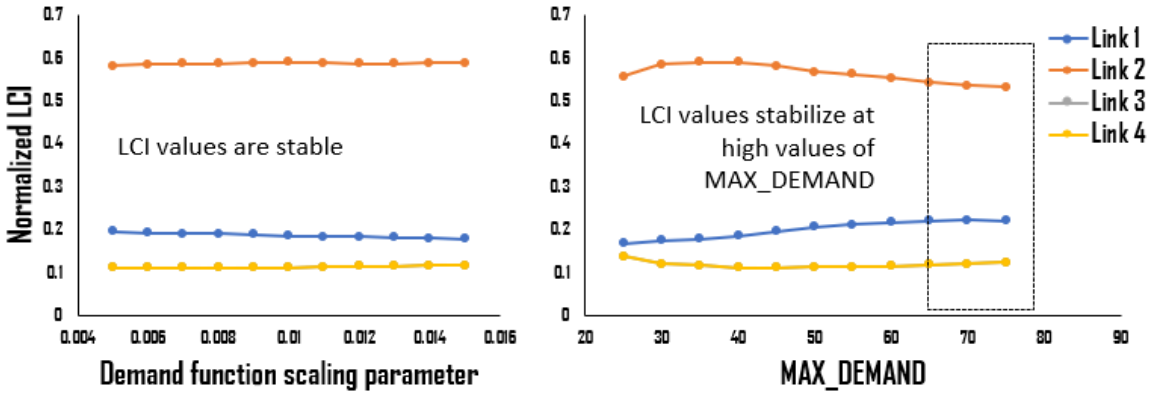

a) Impact of demand function scaling parameter on LCI.

b) Impact of MAX_DEMAND parameter on LCI.

Figure 14. Impact of demand function parameters on LCI.

3.3. Experiment 3: Real-size networks

In this section, two real-size road networks were used to compare the computation time of LCI for different traffic assignment models, and a case study was conducted for bridge criticality assessment in the city of Winnipeg, Manitoba, Canada.

3.3.1 Computational time

The proposed LCI measures were applied to two real-size transportation networks: the Winnipeg and Chicago Sketch networks. These networks were obtained from an open-source repository (*https://github.com/bstabler/TransportationNetworks*). The origins and destinations of the O-D flows were the traffic zones in both networks. Fixed working path sets were used for a fair comparison. The working path set of the Winnipeg network was generated by *Bekhor et al. [36]*, and the working path set of the Chicago sketch network was generated by using a combination of the link elimination method *[55]* and the penalty method *[56]* with a penalty of 5% increase travel time on the links on the shortest path. More details about the test networks are presented in Fig. 15.

154	Zone No.	387
1067	Node No.	933
2,535	Link No.	2,590
4,345	O-D No.	93,135
174,491	Path No.	836,346

Winnipeg

Chicago Sketch

Figure 15. Two real-size transportation networks.

In Table 6, the computational time of LCI for different traffic assignment models on the two test networks is provided. It reports the average CPU time per iteration for solution algorithm steps and computation of LCI scores. The solution algorithm (Section 2.3) was terminated either when RMSE=1e-7 or the maximum iteration number was reached (i.e., 500 iterations). The solution algorithm was implemented in Python 3.7.12. The numerical experiments were conducted on a Microsoft Windows 11 operating system with Intel(R) Core (TM) i7-9700 CPU @ 3.00GHz with 24 GB of RAM.

Table 6. Computational time.

LCI model	Winnipeg					Chicago Sketch				
	Iter. No.	Alg. iter. time (sec)	LCI comp. time (sec)	Total time (min)	Total time with LCI (min)	Iter. No.	Alg. iter. time (sec)	LCI comp. time (sec)	Total time (min)	Total time with LCI (min)
LCI-SUE	116	3.68	5.96	7	19	106	9.49	12.59	17	39
LCI-SUE-ED	243	3.66	6.09	15	40	208	9.67	12.94	34	78
LCI-UE*	500	3.25	6.08	27	78	500	7.74	13.0	65	173
LCI-UE-ED*	500	3.32	6.03	28	78	500	7.74	12.8	65	171

** Reached maximum iteration number*

As shown in Table 6, the solution algorithm for SUE framework converged in about half the iterations as the SUE-ED framework. This was expected because the ED extension added non-linearity to the objective function, increased the number of decision variables (i.e., one extra demand variable for each O-D pair), and increased the number of constraints. The CPU times for these frameworks were proportional to the iterations. The SUE model took 7 minutes for the Winnipeg network and 17 minutes for the Chicago Sketch network. The SUE-ED model took 15 and 35 minutes, respectively. Computing the LCI metric added some extra time, resulting in a total CPU time of 19 minutes for the Winnipeg network and 39 minutes for the Chicago Sketch network for SUE, and 40 and 78 minutes, respectively, for SUE-ED.

Both UE and UE-ED algorithms failed to converge within 500 iterations for both networks. They exceeded the maximum iterations without meeting the RMSE criterion of 1e-7 (although they achieved RMSE=1e-5). The total CPU time for computing LCI values was 78 minutes for the Winnipeg network and 171 minutes for the Chicago Sketch network. The convergence rate of the UE-based TA algorithm was expected to be slower than that of the SUE-based TA algorithm, despite sharing the same solution framework (i.e., flow update strategy and step size determination scheme). This is attributed to the all-

or-nothing (AON) loading procedure employed by the UE-based TA algorithm to obtain a search direction. The AON procedure assigns flows to shortest paths and may result in unbalanced solutions that require further iterations. Conversely, the SUE-based TA algorithm applied a multi-path loading procedure based on a route choice model (i.e., the MNL model) as the search direction to simultaneously allocate flows to multiple paths, which may result in more balanced solutions.

We should emphasize that a full-scan approach for identifying critical links for the same networks would require exponentially more time than the LCI approach. For example, the Winnipeg network has 2,535 links. A full-scan method with the SUE framework would need to multiply the total CPU time by this number, resulting in 7×2535=17,745 minutes (or 296 hours or 11 days).

3.3.2 A case study: The criticality of bridges in the city of Winnipeg

In this section, the bridge criticality in Winnipeg, Manitoba, Canada (Fig. 16) was evaluated. We used the proposed SUE-based LCI measures and compared them with the J-C method by *Jansuwan and Chen (2015)*. We chose the J-C method because it is the only known full-scan method that uses a SUE traffic assignment framework. Table 8 summarizes the top-10 critical bridges according to each measure. Fig. 17 shows the Spearman's rank correlation coefficients between the measures. Appendix B lists the criticality values and rankings for all bridges. We note that there is no ground truth for the bridge criticality values for the Winnipeg network. Therefore, we just compare how the measures reflect the network's functional aspects and traffic flow characteristics.

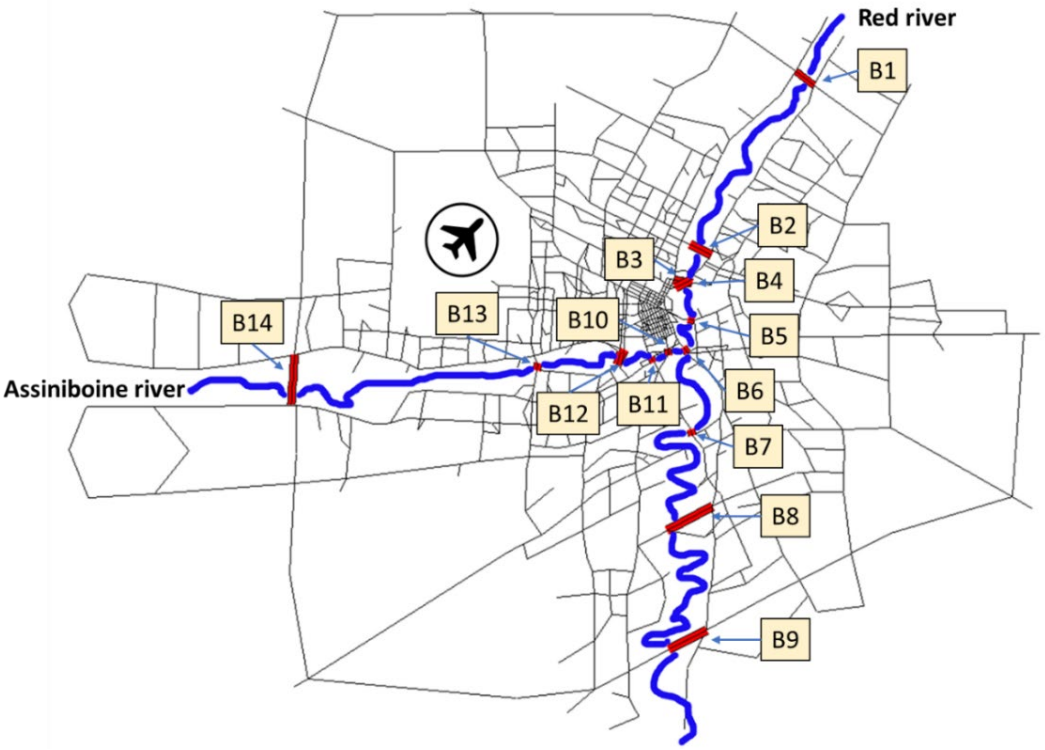

Figure 16. The Winnipeg network and major bridge locations (B1-B14).

The mapping between bridge IDs and their names is provided in Table 7.

Table 7. List of bridges.

Bridge index	*Bridge name*	*Bridge index*	*Bridge name*
B1	*North Perimeter*	*B8*	*Fort Gary*
B2	*Kildonan Settlers*	*B9*	*South Perimeter*
B3	*Redwood*	*B10*	*Mid Town*
B4	*Disraeli*	*B11*	*Osborne*
B5	*Provencher*	*B12*	*Maryland*
B6	*Norwood*	*B13*	*St. James*
B7	*St. Vital*	*B14*	*West Perimeter*

According to Table 8, the most important directional routes are northbound Assiniboine River and westbound Red River, as they carry traffic out of Winnipeg City during the PM peak period. LCI-SUE-ED identified the top three bridges as B13-St. James Bridge (NB), B11-Osborne Bridge (NB), and B5-Provencher Bridge (WB), with St. James Bridge ranked as the most important. Although not the most congested and located outside the city center, it serves as a crucial access point between the airport and residential areas. Any disruption in the NB direction could have an adverse impact on expected travel costs and demands. B11 and B5 are located near the central business district (CBD), which is sensible.

Table 8. Top-10 critical rank bridges of Winnipeg.

	LCI-SUE-ED		*LCI-SUE*		*Original LCI-UE*		*J-C*	
Rank	*Bridge*	*Bound*	*Bridge*	*Bound*	*Bridge*	*Bound*	*Bridge*	*Bound*
1	*B13*	*NB*	*B11*	*NB*	*B10*	*NB*	*B13*	*NB*
2	*B11*	*NB*	*B13*	*NB*	*B11*	*NB*	*B6*	*WB*
3	*B5*	*WB*	*B10*	*NB*	*B4*	*WB*	*B5*	*WB*
4	*B10*	*NB*	*B6*	*WB*	*B5*	*WB*	*B12*	*NB*
5	*B6*	*WB*	*B5*	*WB*	*B13*	*NB*	*B1*	*WB*
6	*B4*	*WB*	*B4*	*WB*	*B6*	*WB*	*B4*	*WB*
7	*B7*	*WB*	*B7*	*WB*	*B12*	*NB*	*B7*	*WB*
8	*B2*	*WB*	*B2*	*WB*	*B11*	*SB*	*B10*	*NB*
9	*B11*	*SB*	*B11*	*SB*	*B3*	*WB*	*B14*	*SB*
10	*B12*	*NB*	*B13*	*SB*	*B13*	*SB*	*B7*	*EB*

LCI-SUE-ED also included B10-Mid Town (NB) and B6-Norwood (WB) into Top-5 ranked bridges. These bridges are near the center similar to J-C method.

In Fig. 17, an aggregated comparison of the bridge criticality rankings obtained by different methods is provided in the form of Spearman's rank correlation.

$$r_{X,Y} = \frac{Cov\big(R(X), R(Y)\big)}{Var\big(R(X)\big)Var\big(R(Y)\big)} \tag{18}$$

where $R(t)$ shows the rank of the observation of t in X or Y data sets. The Spearman's rank correlation takes values in the range from -1 to 1. The positive correlation signifies that the ranks of both the variables are increasing. In contrast, the negative correlation shows that as the rank of one variable increases, the

rank of the other decreased. To be consistent with *[20]*, the strength of the correlation between two variables is categorized as follows: 0 to 0.19 very weak; 0.2 to 0.39 weak; 0.4 to 0.59 moderate; and 0.6 to 0.79 strong; and 0.8 to 1 very strong.

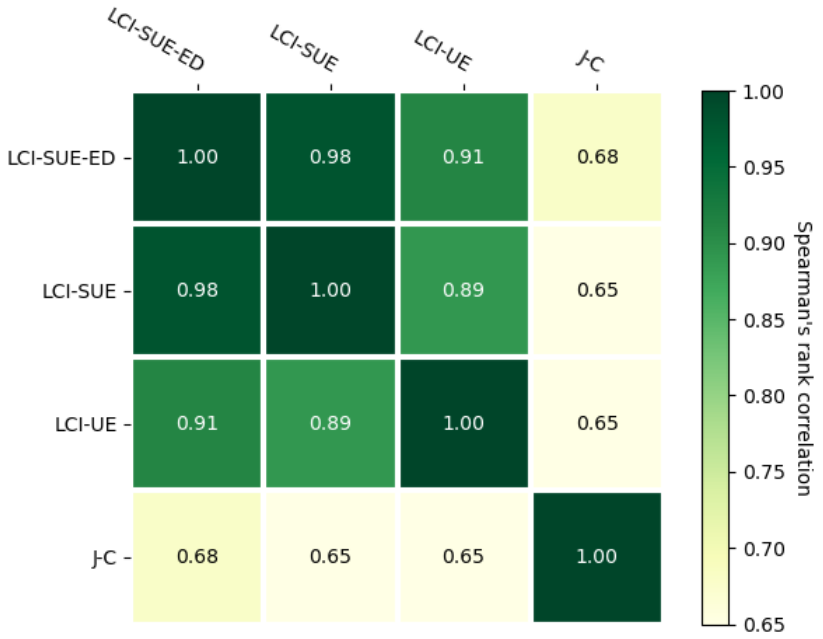

Figure 17. Spearman's rank correlation coefficients.

Fig. 17 shows that all four measures have positive correlations. The LCI measures are strongly correlated with each other and with the J-C measure. The LCI-SUE-ED and J-C measures have the highest correlation, which means that the LCI approach gives a similar ranking to the J-C method. However, we should remember that there is no ground truth for bridge criticality, so we cannot say that one measure is better than another.

4. CONCLUSION

In this study, the functional form of the UE-based LCI was refined to address the zero-flow problem, should an analyst opt to maintain the UE framework. This adjustment enabled the elimination of the contribution of O-D pairs to link criticality when the latter did not carry their flows, thus preventing link criticality overestimation. Subsequently, the analysis was extended to SUE to overcome the limitations of the UE framework. This extension accounted for the stochastic nature of traveler route selection, naturally addressing zero-flow and inconsistent ranking of identical links issues. The zero-flow issue was mitigated by assigning non-zero flows to all paths within a path set based on route choice probabilities. The inconsistency in ranking identical links was resolved by granting equal choice probabilities to paths of an O-D pair with matching travel times in the SUE framework, thereby ensuring an equal distribution of flow (provided these links were not shared with paths of other O-D pairs). Next, the SUE framework was further expanded to the SUE-ED framework, incorporating the potential influence of travel decisions such as travel, destination, or mode choice. The results suggest that SUE-ED facilitated an enhancement of LCI

values for genuinely critical links. Finally, the LCI-SUE and LCI-SUE-ED applied to a real-world transport network for assessing criticality of bridges in the City of Winnipeg, Canada. The results were reasonable and demonstrated coherence with previous methodologies.

The analysis provided in this study used a SUE framework with a simple route choice model. Future work could focus on incorporating advanced route choice models that would be capable of handling route choice correlations *[35, 36, 37]*, travelers' perception variance with respect to path lengths *[26]*, or bounded rationality *[34]*. It would be interesting to see how SUE with advanced choice models can affect link criticality assessment. Because LCI is based on TA and an iterative solution method, we believe that it can be applied to other travel modes (e.g., transit, bicycle, pedestrian, etc.) as well as networks with advanced technologies (e.g., mixed flow of connected-autonomous vehicles and human driven vehicles) that make use of a TA model.

ACKNOWLEDGEMENT

The work described in this paper was jointly supported by research grants from the Research Grants Council of the Hong Kong Special Administrative Region, China (PolyU 15222221), the Department of Civil and Environmental Engineering (1-WZ06), and a Studentship from the Research Institute for Sustainable Urban Development at the Hong Kong Polytechnic University.

REFERENCES

[1] Liu W, Song Z. Review of studies on the resilience of urban critical infrastructure networks. Reliability Engineering & System Safety 2020; 193, 106617.

[2] Boakye J, Guidotti R, Gardoni P, Murphy C. The role of transportation infrastructure on the impact of natural hazards on communities. Reliability Engineering & System Safety 2022; 219, 108184.

[3] Chen BY, Lam WH, Sumalee A, Li Q, Li ZC. Vulnerability analysis for large-scale and congested road networks with demand uncertainty. Transportation Research Part A: Policy and Practice 2012; 46(3), 501-516.

[4] Huang W, Zhou B, Yu Y, Yin D. Vulnerability analysis of road network for dangerous goods transportation considering intentional attack: Based on cellular automata. Reliability Engineering & System Safety 2021; 214, 107779.

[5] Yu YC, Gardoni P. Predicting road blockage due to building damage following earthquakes. Reliability Engineering & System Safety 2022; 219, 108220.

[6] Bucar RC, Hayeri YM. Quantitative assessment of the impacts of disruptive precipitation on surface transportation. Reliability Engineering & System Safety 2020; 203, 107105.

[7] He Z, Navneet K, van Dam W, Van Mieghem P. Robustness assessment of multimodal freight transport networks. Reliability Engineering & System Safety 2021; 207, 107315.

[8] Wandelt S, Shi X, Sun X. Estimation and improvement of transportation network robustness by exploiting communities. Reliability Engineering & System Safety 2021; 206, 107307.

[9] Sullivan JL, Novak DC, Aultman-Hall L, Scott DM. Identifying critical road segments and measuring system-wide robustness in transportation networks with isolating links: A link-based capacity-reduction approach. Transportation Research Part A: Policy and Practice 2010; 44(5), 323-336.

[10] Gu Y, Fu X, Liu Z, Xu X, Chen A. Performance of transportation network under perturbations: Reliability, vulnerability, and resilience. Transportation Research Part E: Logistics and Transportation Review 2020; 133, 101809.

[11] Mylonas C, Mitsakis E, Kepaptsoglou K. Criticality analysis in road networks with graph-theoretic measures, traffic assignment, and simulation. Physica A: Statistical Mechanics and its Applications 2023; 629, 129197.
[12] Jansuwan S, Chen A. Considering perception errors in network efficiency measure: An application to bridge importance ranking in degradable transportation networks. Transportmetrica 2015; 11 (9): 793-818.
[13] Cats O, Jenelius E. Beyond a complete failure: The impact of partial capacity degradation on public transport network vulnerability. Transportmetrica B: Transport Dynamics 2018; 6(2), 77-96.
[14] Ryu S, Chen A, Su J, Choi K. Two-stage bicycle traffic assignment model. Journal of Transportation Engineering, Part A: Systems 2018; 144(2), 04017079.
[15] Lilasathapornkit T, Rey D, Liu W, Saberi M. Traffic assignment problem for footpath networks with bidirectional links. Transportation Research Part C: Emerging technologies 2022; 144, 103905.
[16] Wang X, Renne JL. Socioeconomics of Urban Travel in the US: Evidence from the 2017 NHTS. Transportation Research Part D: Transport and Environment 2023; 116, 103622.
[17] Sheffi Y. Urban transportation networks: Equilibrium analysis with mathematical programming methods. Englewood Cliffs, NJ: Prentice-Hall; 1985.
[18] Almotahari A, Yazici MA. A link criticality index embedded in the convex combinations solution of user equilibrium traffic assignment. Transportation Research Part A: Policy and Practice 2019; 126: 67-82.
[19] Nagurney A, Qiang Q. A transportation network efficiency measure that captures flows, behavior, and costs with applications to network component importance identification and vulnerability. In Proceeding of the POMS 18th Annual Conference 2007; 1–22.
[20] Almotahari A, Yazici MA. A computationally efficient metric for identification of critical links in large transportation networks. **Reliability Engineering & System Safety** 2021; 209: 107458.
[21] Knoop VL, Snelder M, van Zuylen HJ, Hoogendoorn SP. Link-level vulnerability indicators for real-world networks. Transportation Research Part A: Policy and Practice 2012; 46(5), 843-854.
[22] Jung S, Lee S, Kwon O, Kim B. Grid-based traffic vulnerability analysis by using betweenness centrality. Journal of the Korean Physical Society 2020; 77, 538-544.
[23] Gauthier P, Furno A, El Faouzi NE. Road network resilience: How to identify critical links subject to day-to-day disruptions. Transportation Research Record 2018; 2672(1), 54-65.
[24] Yang H, Bell MGH. Models and algorithms for road network design: A review and some new developments. Transport Reviews 1998; 18 (3): 257-278.
[25] Cantarella GE, De Luca S, Di Gangi M, Di Pace R. Stochastic equilibrium assignment with variable demand: Literature review, comparisons, and research needs. WIT Transactions on the Built Environment, Urban Transport 2013; 19 (130): 349–364.
[26] Kitthamkesorn S, Chen A, Xu X. Elastic demand with weibit stochastic user equilibrium flows and application in a motorised and non-motorised network. Transportmetrica A 2015; 11 (2): 158-185.
[27] Fisk C. Some developments in equilibrium traffic assignment. Transportation Research Part B: Methodological 1980; 14 (3): 243-255.
[28] Mattsson LG, Jenelius E. Vulnerability and resilience of transport systems – a discussion of recent research. Transportation Research Part A: Policy and Practice 2015; 81: 16-34.
[29] Zhou Y, Wang J, Yang H. Resilience of transportation systems: Concepts and comprehensive review. In IEEE Transactions on Intelligent Transportation Systems 2019; 20 (12): 4262-4276.
[30] Pan S, Yan H, He J, He Z. Vulnerability and resilience of transportation systems: A recent literature review. Physica A: Statistical Mechanics and its Applications 2021; 581: 126235.
[31] Hassan SA, Amlan HA, Alias NE, Abd Kadir MA, Sukor NSA. Vulnerability of road transportation networks under natural hazards: A bibliometric analysis and review. International Journal of Disaster Risk Reduction 2022; 103393.

[32] Faturechi R, Miller-Hooks E. Measuring the performance of transportation infrastructure systems in disasters: A comprehensive review. ASCE Journal of Infrastructure Systems 2015; 21 (1): 1–15.
[33] Du Y, Wang H, Gao Q, Pan N, Zhao C, Liu C. Resilience concepts in integrated urban transport: A comprehensive review on multi-mode framework. Smart and Resilient Transportation 2022; 4 (2): 104-133.
[34] Duncan LC, Watling DP, Connors RD, Rasmussen TK, Nielsen OA. A bounded path size route choice model excluding unrealistic routes: Formulation and estimation from a large-scale GPS study. Transportmetrica A: Transport Science 2022; 18(3), 435-493.
[35] Prashker J, Bekhor S. Route choice models used in the stochastic user equilibrium problem: A review. Transport Reviews 2004; 24 (4): 437–463.
[36] Bekhor S, Toledo T, Prashker JN. Effects of choice set size and route choice models on path-based traffic assignment. Transportmetrica 2008; 4 (2): 117-133.
[37] Chen A, Pravinvongvuth S, Xu X, Ryu S, Chootinan P. Examining the scaling effect and overlapping problem in logit-based stochastic user equilibrium models. Transportation Research Part A: Policy and Practice 2012; 46(8), 1343-1358.
[38] Prato CG. Route choice modeling: Past, present, and future research directions. Journal of choice modelling 2009; 2(1), 65-100.
[39] Di X, Liu HX. Boundedly rational route choice behavior: A review of models and methodologies. Transportation Research Part B: Methodological 2016; 85, 142-179.
[40] Kazagli E, Bierlaire M, Flötteröd G. Revisiting the route choice problem: A modeling framework based on mental representations. Journal of choice modelling 2016; 19, 1-23.
[41] Alizadeh H, Farooq B, Morency C, Saunier N. On the role of bridges as anchor points in route choice modeling. Transportation 2018; 45(5), 1181-1206.
[42] Ma J, Meng Q, Cheng L, Liu Z. General stochastic ridesharing user equilibrium problem with elastic demand. Transportation Research Part B: Methodological 2022; 162, 162-194.
[43] Wang J, Peeta S, He X. Multiclass traffic assignment model for mixed traffic flow of human-driven vehicles and connected and autonomous vehicles. Transportation Research Part B: Methodological 2019; 126, 139-168.
[44] Huang Y, Kockelman KM. Electric vehicle charging station locations: Elastic demand, station congestion, and network equilibrium. Transportation Research Part D: Transport and Environment 2020; 78, 102179.
[45] Latora V, Marchiori M. Efficient behavior of small-world networks. Physical Review Letters 2001; 87 (19): 198701. https://doi.org/10.1103/PhysRevLett. 87.198701.
[46] Dong S, Gao X, Mostafavi A, Gao J, Gangwal U. Characterizing resilience of flood-disrupted dynamic transportation network through the lens of link reliability and stability. Reliability Engineering & System Safety 2023; 232, 109071.
[47] Jenelius E, Petersen T, Mattsson L. Importance and exposure in road network vulnerability analysis. Transportation Research Part A: Policy and Practice 2006; 40 (7): 537–560.
[48] Almotahari A, Yazici A. Impact of topology and congestion on link criticality rankings in transportation networks. Transportation Research Part D: Transport and Environment 2020; 87, 102529.
[49] Liu Z, Chen H, Liu E, Hu W. Exploring the resilience assessment framework of urban road network for sustainable cities. Physica A: Statistical Mechanics and its Applications 2022; 586, 126465.
[50] Shapouri M, Fuller JD, Wolshon B, Herrera N. Disruptions in megaregional network evacuations: Identifying and assessing critical links. Transportation Research Record 2023; 2677(9), 669–682.
[51] Mahajan K, Kim AM. Vulnerability assessment of Alberta's provincial highway network. Transportation Research Interdisciplinary Perspectives 2020; 6, 100171.
[52] Ohi SJ, Kim AM. Identifying critical corridors during an area-wide disruption by evaluating network bottleneck capacity. International Journal of Disaster Risk Reduction 2021; 64, 102487.

[53] Patriksson M. The traffic assignment problem: Models and methods. Utrecht, The Netherlands: VSP; 1994.
[54] Liu HX, He X, He B. Method of successive weighted averages (MSWA) and self-regulated averaging schemes for solving user equilibrium problem. Networks and Spatial Economics 2009; 9: 485-503.
[55] Azevedo J, Santos Costa MEO, Silvestre Madeira JJER, Vieira Martins EQ. An algorithm for the ranking of shortest paths. European Journal of Operational Research 1993; 69 (1), 97–106.
[56] De La Barra T, Perez B, Anez J. Multidimensional path search and assignment. In Proceedings of the 21st PTRC Summer Annual Meeting 1993; England.

APPENDIX A

In this section, we discuss the applicability of elastic demand (ED) extension of TA to the context of link criticality ranking. We start with a conceptual interpretation and proceed with a sensitivity analysis.

A possible interpretation

We believe that incorporating ED into link criticality assessment can be interpreted as adding another choice dimension to the metric, namely ***trip criticality***. It seems to us that the core question is *whether the link's criticality should vary under different demand levels or remain constant.* The simplest example we could think of is a trip generation choice under normal and degraded conditions in a single-link network. In a degraded network, travel demand may reduce due to the decrease in level of service. Should the criticality of the link reduce with the decrease of travel demand? To answer this question, we consider travel demand from the perspective of individual trips, which we classified as *mandatory* and *discretionary* (or optional) trips. Demand reduction can be interpreted as cancelation of discretionary trips. The following logic can be used: *"If trips are canceled, then people can 'survive' without these trips. If they can survive without these trips, then they may survive without the corresponding connection. If they can survive without this connection, is it critical?".* Following this logic, it seems reasonable to reduce the criticality of links if travel demand reduces. As a result, the ED extension may be considered by incorporating the impact of trip criticality into link criticality assessment. The sensitivity analysis conducted on SUE and SUE-ED showed results are consistent with our intuition.

Sensitivity analysis

To support the above discussion, the impact of ED on a full-scan approach (based on the difference of total network travel time) and LCI is analyzed. The experiments were conducted on a simple three-link network as shown in Fig. 18. The results are summarized in Tables 9 - 11.

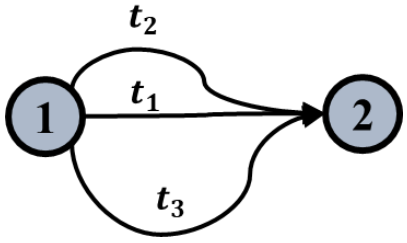

Figure 18. The three-link network.

The travel time of each link is computed according to (14). All characteristics of the three links were set identical except the free flow travel time. The link free flow travel times were set to obey the following relation:

$$t_1^0 < t_2^0 < t_3^0$$

The demand function is calculated according to (15). The SUE and SUE-ED frameworks were selected for the analysis. The solution algorithm described in Section 2.3 was utilized. The link criticality of the full-scan approach was calculated as follows:

$$Criticality_a = \frac{(T_{ALL\ LINKS} - T_a)}{T_{ALL\ LINKS}}, \qquad a = \{1,2,3\}$$

where $Criticality_a$ is the criticality score of link a, $T_{ALL\ LINKS}$ is the total travel time when all links are intact, T_a is the total travel time in which link a is removed. To make the full-scan measure comparable to LCI, we normalize both indices according to (16).

Table 9 provides the link criticality values using the full-scan and LCI-SUE approaches under the fixed demand (FD) TA. The total travel time of a fully functioning network is much lower than the total travel time in disrupted networks. It was expected because the travel demand remained fixed regardless of the degradation of the network. Specifically, the removal of Link 1 (i.e., fastest) resulted in the highest discrepancy than removal of Link 2 (i.e., mediocre) or Link 3 (i.e., slowest) as expected. It was reflected in the link criticality scores. The criticality of Link 1 was almost twice as high as the ranks of other two links. The LCI-SUE followed the same trend but the difference between the criticality scores was lower than for the full-scan method.

Table 9. Link criticality values for SUE-FD.

Scenario	Full-scan				Normalized LCI-SUE
	O-D demand	Total network travel time	Criticality	Normalized Criticality	
Fully functional	11.76	650	-	-	-
Link 1	11.76	3206	3.94	0.47	0.4
Link 2	11.76	2227	2.43	0.29	0.32
Link 3	11.76	2008	2.09	0.25	0.28

Tables 10 and 11 provide the criticality values of the same metrics under the elastic demand (ED) TA under two levels of maximum demand. As shown in Table 10 under $\bar{q} = 20$, the travel demand reduced when the network was degraded. Similarly, the degradation was the highest when Link 1 was removed, mediocre when Link 2 was removed, and the lowest when Link 3 was removed. However, due to the decreased demand, the difference in ratings was less pronounced than in the FD TA shown in Table 9. Compared to the full-scan approach, the LCI-SUE-ED did not change much. These results are consistent with the above interpretation. As for the case with $\bar{q} = 40$ shown in Table 11, the travel demand, total network travel time, and hence link criticality values may depend on the parameter values of the demand function. These parameter values might be set such that the total travel time of a fully functioning network is worse than the travel time in the degraded network. In this case, the link criticality of the full-scan method may have negative values. One can observe that the demand was considerably reduced in these

scenarios. This can be interpreted as a strong suppression of discretionary trips due to the sensitivity of the demand function to travel cost. Based on the negative results, it seems that the full-scan method used in this section is applicable only in scenarios when the demand function is less sensitive to travel cost. In contrast, the LCI values were consistent with the interpretation given above and the elastic demand did not compensate for the metric.

Table 10. Link criticality values for the SUE-ED model with $\bar{q} = \mathbf{2} \cdot q,\ q = 10$.

Scenario	Full-scan				Normalized LCI-SUE-ED
	O-D demand	Total network travel time	Criticality	Normalized Criticality	
Fully functional	11.76	650	-	-	-
Link 1	8.41	740	0.14	0.37	0.4
Link 2	9.133	728	0.12	0.32	0.32
Link 3	9.35	723	0.11	0.30	0.28

Table 11. Link criticality values for the SUE-ED model with $\bar{q} = \mathbf{4} \cdot q,\ q = 10$.

Scenario	Full-scan				Normalized LCI-SUE-ED
	O-D demand	Total network travel time	Criticality	Normalized Criticality	
Fully functional	14.5	**1503.0**	**-**	-	-
Link 1	9.78	**1101.4**	**-0.27**	**-**	0.37
Link 2	10.66	**1424.4**	**-0.05**	**-**	0.33
Link 3	10.92	**1433.1**	**-0.05**	**-**	0.3

APPENDIX B

In this section, we list the criticality values and rankings for all bridges of the Winnipeg network (see Section 3.3.2).

Table 12. Ranking of bridges in the Winnipeg network.

Bridge	*Bound*	*LCI-SUE-ED*	*Rank*	*LCI-SUE*	*Rank*	*Original LCI*	*Rank*	*J-C*	*Rank*
B1	*EB*	*0.000202803*	*27*	*0.000295122*	*27*	*7.32E-05*	*25*	*0.0226*	*22*
B1	*WB*	*0.00077967*	*13*	*0.000693302*	*14*	*0.001049893*	*11*	*0.0394*	*5*
B2	*EB*	*0.000491365*	*18*	*0.000467258*	*20*	*0.000130798*	*22*	*0.0232*	*18*
B2	*WB*	*0.00108921*	*8*	*0.001109025*	*8*	*0.000380973*	*14*	*0.0235*	*17*
B3	*EB*	*0.000516074*	*17*	*0.000463788*	*22*	*0.000300522*	*15*	*0.0269*	*11*
B3	*WB*	*0.000528447*	*16*	*0.000597139*	*17*	*0.001441548*	*9*	*0.0243*	*16*
B4	*EB*	*0.00022502*	*26*	*0.00033371*	*26*	*0.000121963*	*23*	*0.0217*	*24*
B4	*WB*	*0.001901061*	*6*	*0.001871501*	*6*	*0.00444422*	*3*	*0.0339*	*6*
B5	*EB*	*0.000340055*	*21*	*0.000485995*	*19*	*0.000107344*	*24*	*0.0251*	*14*
B5	*WB*	*0.002879879*	*3*	*0.002079427*	*5*	*0.004042402*	*4*	*0.0415*	*3*
B6	*EB*	*0.000598466*	*15*	*0.000673294*	*15*	*0.000145122*	*19*	*0.0166*	*28*
B6	*WB*	*0.002608147*	*5*	*0.002182029*	*4*	*0.002897735*	*6*	*0.0582*	*2*

B7	*EB*	*0.000485164*	*19*	*0.000651325*	*16*	*0.000285303*	*17*	*0.0288*	*10*
B7	*WB*	*0.001400595*	*7*	*0.001228801*	*7*	*0.000632031*	*12*	*0.0335*	*7*
B8	*EB*	*0.000252003*	*25*	*0.000367765*	*25*	*5.46E-05*	*26*	*0.0228*	*21*
B8	*WB*	*0.000899356*	*11*	*0.000764342*	*13*	*0.000565221*	*13*	*0.0251*	*15*
B9	*EB*	*0.000180841*	*28*	*0.000261946*	*28*	*4.90E-05*	*27*	*0.0215*	*25*
B9	*WB*	*0.000262703*	*24*	*0.000393847*	*24*	*4.71E-05*	*28*	*0.0206*	*26*
B10	*NB*	*0.002748177*	*4*	*0.002470014*	*3*	*0.00721885*	*1*	*0.0321*	*8*
B10	*SB*	*0.000419603*	*20*	*0.000535903*	*18*	*0.000182898*	*18*	*0.0197*	*27*
B11	*NB*	*0.002992395*	*2*	*0.003436072*	*1*	*0.004537469*	*2*	*0.0232*	*19*
B11	*SB*	*0.001071524*	*9*	*0.001035884*	*9*	*0.001453956*	*8*	*0.0231*	*20*
B12	*NB*	*0.000968415*	*10*	*0.000843461*	*11*	*0.00207325*	*7*	*0.0411*	*4*
B12	*SB*	*0.000277295*	*23*	*0.000395476*	*23*	*0.000296884*	*16*	*0.0222*	*23*
B13	*NB*	*0.003425651*	*1*	*0.002716636*	*2*	*0.003059365*	*5*	*0.0672*	*1*
B13	*SB*	*0.0008675*	*12*	*0.000930731*	*10*	*0.001244938*	*10*	*0.0266*	*12*
B14	*NB*	*0.000334909*	*22*	*0.000466869*	*21*	*0.000132711*	*21*	*0.0255*	*13*
B14	*SB*	*0.000634739*	*14*	*0.000810078*	*12*	*0.000140812*	*20*	*0.029*	*9*